JPET # 265561

Title Page

Fentanyl but not Morphine Interacts with Non-Opioid Recombinant Human Neurotransmitter Receptors and Transporters

Randy Torralva[a,b,c], Amy J. Eshleman[a,c,d], Tracy L. Swanson[a,c], Jennifer L. Schmachtenberg[a,c], William E. Schutzer[a,c,e], Shelley H. Bloom[a,c], Katherine M. Wolfrum[a,c], John F. Reed[a,c], Aaron Janowsky[a,c,d,e]

[a]Research Service, VA Portland Health Care System, Portland OR USA

[b]Coda Research, Portland OR USA

[c]Department of Psychiatry, Oregon Health & Science University, Portland OR USA

[d]Department of Behavioral Neuroscience, Oregon Health & Science University, Portland OR USA

[e]The Methamphetamine Abuse Research Center, VA Portland Health Care System and Oregon Health & Science University, Portland OR USA

Running Title Page

Running Title: Opioid Interactions with Non-Opioid Receptors

Corresponding author: Aaron Janowsky

Research Service (R&D22), VA Portland Health Care System,

3710 S.W. U.S. Veterans Hospital Rd.

Portland OR 97239

E-mail: janowsky@ohsu.edu

Phone: 503 721-7912

Fax: 503 721-7839

Number of text pages: 20 (includes abstract & intro)

Number of tables: 7

Number of figures: 7

Number of References: 62

Number of words in the Abstract: 250

Number of words in the Introduction: 733

Number of words in the Discussion: 1500

Abbreviations: Adrenoceptor, Adr; α_{1A}-Adr, alpha 1 adrenoceptor subtype A; α_{1B}-Adr, alpha 1 adrenoceptor subtype B; α_{1D}-Adr, alpha 1 adrenoceptor subtype D; CHO, Chinese hamster ovary cells; DA, dopamine; DAMGO, [D-Ala^2, *N*-MePhe^4, Gly-ol]-enkephalin; DAT, dopamine transporter; DHTB, dihydrotetrabenazine; DMEM, Dulbecco's Modified Eagle Medium, DPDPE, [D-Pen^2,D-Pen^5]encephalin; F/FA, fentanyl and fentanyl analogues; FIMR, fentanyl-induced muscular rigidity, FIRE, fentanyl-induced respiratory effects; GPCR, G-protein coupled receptor; GTPɣS, guanosine 5'-O-[gamma-thio]triphosphate); hDOR, human delta opioid receptors; 5-HT,

serotonin; IP-1, inositol-1 phosphate; HEK, human embryonic kidney cells; hKOR, human kappa opioid receptors; LC, locus coeruleus; MK-801 (dizocilpine), (5*S*,10*R*)-(+)-5-Methyl-10,11-dihydro-5*H*-dibenzo[*a*,*d*]cyclohepten-5,10-imine maleate; NE, norepinephrine; NET, norepinephrine transporter; NMDA, N-methyl-D-aspartate; 8-OH-DPAT, 8-hydroxy-2-(di-n-propylamino) tetralin; PEI, polyethylenimine; rMOR, rat mu opioid receptors; RTI-55, methyl (1R,2S,3S)-3-(4-iodophenyl)-8-methyl-8-azabicyclo[3.2.1]octane-2-carboxylate; SCH23390, 7-chloro-3-methyl-1-phenyl-1,2,4,5-tetrahydro-3-benzazepin-8-ol; SERT, serotonin transporter; SKF38393, (±)-1-Phenyl-2,3,4,5-tetrahydro-(1*H*)-3-benzazepine-7,8-diol; U69,593, (+)-(5α,7α,8β)-N-Methyl-N-[7-(1-pyrrolidinyl)-1-oxaspiro[4.5]dec-8-yl]-benzeneacetamide; VMAT2, vesicular monoamine transporter 2; WIN55,212, (R)-(+)-[2,3-Dihydro-5-methyl-3-(4-morpholinylmethyl)pyrrolo[1,2,3-*de*]-1,4-benzoxazin-6-yl]-1-naphthalenylmethanone mesylate.

Recommended Section Assignment: Neuropharmacology

Abstract

Synthetic opioids, including fentanyl and its analogues, have therapeutic efficacy in analgesia and anesthesia. However, their illicit use in the U.S. has increased, and contributed to the number one cause of death for adults 18-50 years old. Fentanyl and the heroin metabolite, morphine, induce respiratory depression that can be treated with the mu opioid receptor (MOR) antagonist, naloxone. With higher or more rapid dosing, fentanyl, more than morphine, causes chest wall rigidity, and can also induce rapid onset laryngospasm. Because non-MORs could mediate differing clinical manifestations, we examined the interactions of fentanyl and morphine at recombinant human neurotransmitter transporters, G protein-coupled receptors, and the NMDA glutamate receptor. Both drugs were agonists at MOR, kappa, and delta opioid receptors. Morphine had little or no affinity at other human receptors and transporters (Ki or IC_{50} value >100μM). However, fentanyl had Ki values of 1,407nM and 1,100nM at α_{1A} and α_{1B} adrenoceptor subtypes, respectively, Ki values of 1,049nM and 1,670nM at dopamine D4.4 and D1 receptor subtypes, respectively, and also blocked [^{3}H]neurotransmitter uptake by the vesicular monoamine transporter 2 (VMAT2) (IC_{50} = 911nM). Pharmacokinetic models indicate that these Ki and IC_{50} values are pharmacologically relevant. Fentanyl had little affinity for other receptors or transporters. Thus, noradrenergic disposition at specific receptor subtypes in relevant organs may play a role in respiratory and cardiothoracic effects of fentanyl. Data suggest that less selective fentanyl receptor pharmacology could play a role in the different clinical effects of morphine compared to fentanyl, including fentanyl-induced deaths following illicit use.

Significance Statement: The synthetic opioid, fentanyl, induces different clinical effects including rapid onset muscular rigidity, vocal cord closure and rapid death, than the heroin metabolite, morphine. Our data indicate for the first time that the two drugs have very different

effects at recombinant human neurotransmitter receptors and transporters that might explain those clinical differences.

Introduction

Fentanyl (N-phenyl-N-[1-(2-phenylethyl)-4-piperidinyl]propanamide), a synthetic opioid, and its analogues (F/FAs) are involved in almost twice as many opioid-induced deaths as heroin (diacetyl morphine), the metabolic precursor of morphine (Jannetto et al., 2019); (Hedegaard, 2018). However, in hospitals, fentanyl use for analgesia and anesthesia is routine (Stanley, 2014). Side effects include respiratory depression that is treated with naloxone, a mu opioid receptor (MOR) antagonist. Additionally, fentanyl-induced severe skeletal muscle rigidity (FIMR) of the chest wall and diaphragm and acute vocal cord closure (laryngospasm) require a muscle relaxant/paralytic and endotracheal intubation to restore adequate ventilation. These fentanyl-induced respiratory effects (FIRE) may play a role in rapid death associated with illicit fentanyl use.

Symptoms of overdose from illicit use of heroin similarly include naloxone-reversible respiratory depression. However, patients who overdose following illicit fentanyl exposure are far less likely to recover even after treatment with naloxone (Slavova et al., 2017), and higher doses of naloxone are generally required (Somerville et al., 2017). This reduced sensitivity to naloxone could be due to non-MOR-related effects of fentanyl and may explain why deaths from F/FAs continue to increase (Baumann et al., 2018). In fact, naloxone in higher doses causes non-cardiogenic pulmonary edema (Jiwa et al., 2018), exacerbating respiratory failure and non-MOR-mediated symptoms of opioid overdose. Rapidity of injection and dose of fentanyl are the key determinants of the incidence, severity and duration of FIRE (Grell et al., 1970). Symptoms occur within 2 minutes of drug injection and can last up to 15 minutes (Scamman, 1983; Streisand et al., 1993). Fentanyl's inactive metabolite, norfentanyl, appears in plasma within 90

JPET Fast Forward. Published on June 8, 2020 as DOI: 10.1124/jpet.120.265561
This article has not been copyedited and formatted. The final version may differ from this version.

seconds of a bolus intravenous injection (McClain and Hug, 1980), but little norfentanyl is found in autopsy tissue from overdose deaths due to fentanyl (Burns et al., 2016). The absence of metabolite suggests that death from a bolus injection of fentanyl is rapid, distinguishing it from respiratory depression following heroin overdose.

Complex fentanyl pharmacokinetics vary across compartments (plasma, CSF, brain lipid) (Peng and Sandler, 1999). Although fentanyl plasma concentrations are much lower than brain lipid concentrations (Chesser et al., 2019), the high lipid solubility and rapidity of exposure to the CNS following high dose fentanyl suggests that micromolar Ki values for fentanyl binding to non-MORs could be relevant under toxic conditions (Stone and DiFazio, 1988; Yamanoue et al., 1993; Hustveit, 1994).

Descriptions of non-opioid receptor pharmacology i.e., direct interaction between morphine or fentanyl and human signal transduction proteins, which could be linked to the disparate clinical effects of fentanyl and morphine are sparse (see PDSP database: https://pdsp.unc.edu/databases/pdsp.php). Locus coeruleus (LC) activation may play a role in FIMR and FIRE, and multiple animal studies suggest that fentanyl interacts with α_1-adrenoceptors (Adrs) (Lui et al., 1989; Tsou et al., 1989; Lui et al., 1990; Fu et al., 1997). Additionally fentanyl interacts with the human dopamine transporter *in vivo* (Bergstrom et al., 1998), and fentanyl displaces [^{3}H]8-hydroxy-2-(di-n-propylamino) tetralin (8-OH-DPAT) from serotonin (5-HT) 1A receptors in rat brain preparations (Martin et al., 1991) and transfected cells (Rickli et al., 2018). Finally, fentanyl but not morphine interacts with the human ether a-go-go-related gene potassium channel (Katchman et al., 2002; Tschirhart et al., 2019), which could play a role in fentanyl-mediated rapid changes in cardiovascular function.

Data described herein are the first to show that morphine has low affinity (Ki ~100 µM) at the examined recombinant human non-opioid receptors and transporters, while fentanyl has high nanomolar or low micromolar Ki or IC_{50} values for displacing radioligand binding or

antagonizing function at specific recombinant human α_1-Adr subtypes, the vesicular monoamine transporter (VMAT2), and the dopamine D1 and D4.4 receptor subtypes. Further, carfentanil, a potent fentanyl analogue, had binding affinities similar to fentanyl for α_1-Adr subtypes. Conversely, Ki values for fentanyl at displacing radioligand binding at serotonin 1A, 2A, 2B, 2C, dopamine D2 and D3, cannabinoid CB1, and N-methyl-D-aspartate (NMDA) G2a/G1 receptors and at dopamine (DAT), norepinephrine (NET) and serotonin (SERT) transporters, were in the high micromolar range. Additionally, we investigated the effects of fentanyl on receptor and transporter function where fentanyl binding affinity was pharmacologically relevant, and the data indicate that fentanyl is an inhibitor/antagonist of function. These data suggest that there are significant differences between morphine and fentanyl pharmacology. This, along with previously published results indicating that the effects of F/FAs on animal models of FIMR and FIRE can be blocked with non-MOR antagonists, point to new directions for the development of treatments for the effects of synthetic opioids.

Materials and Methods:

Drugs and chemicals

Fentanyl, carfentanil, morphine and naloxone were obtained from the Drug Supply Program, National Institute on Drug Abuse (Rockville, MD). Norepinephrine, epinephrine, phenylephrine, prazosin and tamsulosin were obtained from Sigma-Aldrich Chemical Co. (St. Louis, MO).

[^{3}H] 8-OH-DPAT, [^{3}H]7-chloro-3-methyl-1-phenyl-1,2,4,5-tetrahydro-3-benzazepin-8-ol (SCH23390), [^{125}I]methyl (1*R*,2*S*,3*S*)-3-(4-iodophenyl)-8-methyl-8-azabicyclo[3.2.1]octane-2-carboxylate) (RTI-55), [^{3}H]dopamine, [^{3}H]5HT, [^{3}H]prazosin, [^{3}H]spiperone, [^{3}H]CP-55,940, [^{3}H]MK-801, [^{3}H]dihydrotetrabenazine, and [^{3}H]norepinephrine, were purchased from Perkin Elmer Life and Analytical Sciences (Boston, MA).

JPET Fast Forward. Published on June 8, 2020 as DOI: 10.1124/jpet.120.265561
This article has not been copyedited and formatted. The final version may differ from this version.

All other commonly used reagents were obtained from commercial sources except where specified.

Tissue culture:

Human embryonic kidney cells (HEK-293) or Chinese hamster ovary (CHO) cells were cultured and transfected with the respective recombinant human receptor, rat receptor (MOR), or human transporter using modifications of previously described methods (Eshleman et al., 1999; Eshleman et al., 2013).

Receptor binding assays: Radioligand binding to the VMAT2 (Eshleman et al., 2013; Provencher et al., 2018), dopamine D1, D2, D3, and D4.4 receptors (Eshleman et al., 2013; Janowsky et al., 2014), 5-HT 1A, 2A, 2B, and 2C receptors (Eshleman et al., 2013; Eshleman et al., 2018), and the dopamine, norepinephrine, and serotonin transporters (Eshleman et al., 1999; Eshleman et al., 2013) were conducted as previously described. Methods used to examine drug interactions with additional receptors are described below.

α_1-Adr subtypes: To characterize opioid and other drug interactions with the alpha 1 adrenergic receptor subtypes, human embryonic kidney cells expressing the recombinant human α_{1A} adrenergic receptor (HEK-α_{1A}-Adr), human α_{1B} adrenergic receptor (HEK-α_{1B}-Adr) or the human α_{1D} adrenergic receptor (HEK-α_{1D}-Adr) were grown in Dulbecco's Modified Eagle Medium (DMEM) supplemented with 10% Fetal Clone, 300 µg/ml G418, and 0.05% penicillin/streptomycin. The source and plasmid for the receptor cDNAs were: Bloomsburg University cDNA Resource Center, pcDNA3.1+ (α_{1A}-Adr, α_{1B}-Adr) and α_{1D}-Adr (Genscript, pcDNA3.1+). HEK-293 cells were stably transfected using modifications of our previously described methods (Shi et al., 2016).

Confluent cells (150mm plate) were rinsed with phosphate-buffered saline (PBS), scraped into PBS, centrifuged for 10 min at 1000xg 4^{o}C. The pellet was resuspended and polytronned in Tris buffer (pH 7.4 @ 4^{o}C) and centrifuged at 30,000xg for 15 min, 4^{o}C. The Tris

JPET Fast Forward. Published on June 8, 2020 as DOI: 10.1124/jpet.120.265561
This article has not been copyedited and formatted. The final version may differ from this version.

wash was repeated. Cells were resuspended in 3 ml Tris and stored at -80ºC until needed. The binding assay, adapted from published methods (Yang et al., 1998), was performed in duplicate in a 96-well plate. Serial dilutions of test compounds were made using the Biomek 4000 robotics system (Beckman Coulter, Brea CA), and assay buffer (50 mM Tris buffer, pH 7.4 at 25ºC, containing 0.2 mg/ml ascorbic acid and 100 µM tropolone). The resuspension volumes for each cell line were α_{1A}-Adr: 1 plate/~6.5 ml buffer, α_{1B}-Adr: 1 plate/10 ml buffer, α_{1D}-Adr: 2 plates/6.5 ml buffer. Membranes were preincubated with drugs for 10 min prior to addition of [^{3}H]prazosin (1-2 nM final conc., 80 Ci/mmol, Perkin Elmer) in a final volume of 250 µl. Nonspecific binding was defined with 10 µM phentolamine. The reaction was incubated for 45 min at 25ºC and terminated by filtration over 0.05% PEI- soaked “A” filtermats using cold Tris buffer (50 mM, pH 7.4) with a 6 sec wash. Validation compounds included norepinephrine, epinephrine, phenylephrine, prazosin, phentolamine, and tamsulosin. The filters were dried, spotted with scintillation cocktail, and counted for 2 min after a 4 hr interval, on a Perkin Elmer microbetaplate counter.

Opioid Receptor Subtypes: To characterize drug effects on radioligand binding to human delta, and kappa opioid receptors (DORs and KORs, respectively) transfected into Chinese hamster ovary (CHO) cells (provided by SRI) and rat MOR transfected into CHO cells (provided by Dr. Thomas Murray), cell lines were maintained in Dulbecco's minimal essential medium (DMEM) supplemented with 10% FBS, 400 µg/mL G418, and 0.1% penicillin/streptomycin. All cell lines were grown to confluence, then harvested for membrane preparation. The membranes for binding assays were prepared in 50 mM Tris buffer (pH 7.5 at 4ºC). Cells were scraped from the plates in cmf-PBS and centrifuged at 500 x *g* for 15 min. The cell pellet was homogenized in 2 ml buffer with a polytron, diluted with 11 ml buffer, and centrifuged at 40,000 x *g* for 15 min, washed and recentrifuged. The final pellet was covered with 3 ml buffer and stored at -80ºC until needed.

Binding assays were conducted using [^{3}H]DAMGO, [^{3}H]DPDPE (0.8 nM, ~20,000 cpm)**,** and [^{3}H]U69,593 (0.8 nM, ~22,000 cpm) at the MORs, DORs, and KORs, respectively. The assays were performed in duplicate in 96-well plates using 50 mM Tris buffer (pH 7.7 at room temp). Nonspecific binding was determined with 1.0 µM of the unlabeled analogue of each radioligand. Cell membranes were incubated with the appropriate radioligand and test compound at 25˚C for 60 min. The incubation was terminated by rapid filtration through Perkin Elmer Filtermat A filters presoaked in 0.05% polyethylenimine on a Tomtec cell harvester, and bound radioactivity determined as described for other receptors, above. For [^{3}H]DAMGO, [^{3}H]DPDPE and [^{3}H]U69,593, the Kd values are 0.147, 0.789 and 0.65 nM, respectively. The densities of receptors are 0.373 ± 0.095, 32.8 ± 1.7 and 11.29 ± 0.34 pmol/mg protein for the MOR, DOR, and KOR cell lines, respectively.

CB1 Cannabinoid Receptor: The method for [^{3}H]CP-55,940 binding assays was adapted from (Farrens et al., 2002). The source and plasmid for the receptor cDNA was cDNA Resource Center (Bloomsburg, Pa), pcDNA3.1+. HEK-293 cells were transfected using lipofectamine 2000 (Invitrogen). WIN 55,212 (10 µM) was used to define nonspecific binding. HEK-CB1 cells were grown until confluent on 15 cm dishes. Cells were scraped into 7 ml cmf-PBS, and centrifuged at 11,000xg for 10 min. The supernatant was decanted, and the pellet was resuspended with a Polytron in 5 ml hypotonic buffer (5 mM Tris, 2 mM EDTA + protease inhibitors (PI)). The homogenate was centrifuged at 35,000 x g for 20 min, resuspended in TME buffer with PI (20 mM Tris, 5 mM MgCl2, 1 mM EDTA, pH 7.4 at 4^{o}C with PI) using a Polytron. Following centrifugation at 35,000xg for 20 min, the pellet was resuspended in TME+PI buffer (1.6-3 ml for competition or saturation binding assay) using a Polytron. Proteins were quantified using the BCA kit (ThermoFisher, Waltham MA).

Binding assays used TME supplemented with 5 mg bovine serum albumin (BSA)/ml, pH 7.4 at 30^{o}C. The reaction included test compounds or WIN-55,212, membrane preparation (15-

JPET Fast Forward. Published on June 8, 2020 as DOI: 10.1124/jpet.120.265561
This article has not been copyedited and formatted. The final version may differ from this version.

70 ug, depending on the expression level of CB1), [^{3}H]CP-55,940, and TME+BSA buffer to a final volume of 0.5 ml. In saturation binding assays, the range of concentrations of [^{3}H]CP-55,940 was 0.07-3 nM. In competition binding assays, the concentration of [^{3}H]CP-55,940 was 1.2-1.5 nM. After incubation at 30^{o}C for 60 min, the reaction was terminated by filtration with TME + 1 mg BSA/ml over Filtermat A filters presoaked in 0.2% polyethylenimine. An additional wash was added to the normal harvesting program to reduce nonspecific binding.

NMDA receptor binding: The methods were adapted from (Grant et al., 1997). For functional NMDA receptors, cells need to express two NMDA receptor subunits, the GluN1a and the GluN2a. However, simultaneous and stable expression of both subunits is toxic to the cell ((Grant et al., 1997) and personal observation). We developed a method using a cell line that stably expresses one of the subunits (GluN2a), and that is subsequently transfected with the cDNA for the other subunit (GluN1a) the week of the experiment.

HEK cells stably expressing the GluN2a subunit (G2a-Myc cDNA, Origene) were transfected with 10 µg of Grin1-tGFP cDNA (Origene) using the polyethylenimine (PEI) as we have previously described (Shi et al., 2016). On day 2, medium was changed to DMEM supplemented with selection antibiotic G418 (300 µg/ml). To reduce co-expression toxicity, the receptors were blocked with 100 µM ketamine (adapted from (Grant et al., 1997) and incubated for 48 hr. On day 4, cells were harvested by pouring off the medium, rinsing with 10 ml HEPES buffer (20 mM), and each plate of cells was scraped into 10 ml of high Mg2+ buffer (20 mM HEPES, 100 µM glycine, 100 µM glutamate, 300 µM MgCl2, pH 7.5). To remove the ketamine, cells were incubated for 30 min at 32^{o}C, centrifuged for 10 min at 48,000 x g at 4^{o}C. EDTA buffer (20 mM HEPES, 1 mM EDTA, pH 7.5) was added, the pellet was homogenized using a Polytron, and the membranes were incubated for 30 min at 32^{o}C. Following centrifugation, the pellet was polytronned in ~3 ml assay buffer (20 mM HEPES, 100 µM glycine, 100 µM glutamate, 100 µM MgCl2, 0.2 mg/ml ascorbic acid, pH 7.5).

JPET Fast Forward. Published on June 8, 2020 as DOI: 10.1124/jpet.120.265561
This article has not been copyedited and formatted. The final version may differ from this version.

The binding assay included drug, membrane preparation, [^{3}H]MK-801 (~20 nM) and assay buffer in a final volume of 250 µl. Specific binding was defined as the difference between total binding and nonspecific binding in the presence of 10 µM unlabeled MK-801. The reaction was incubated for 60 min at 22^{o}C, and terminated by filtration with ice cold 20 mM HEPES buffer, pH 7.5 through Perkin Elmer A filtermats presoaked in 0.5% polyethylenimine using a Tomtec 96-well harvester. Radioactivity remaining on filters was counted in a Perkin Elmer microbetaplate reader.

Assays of Function

Assays of VMAT2 function (Eshleman et al., 2013; Provencher et al., 2018), dopamine D1 and D4.4 receptor function (Eshleman et al., 2013; Janowsky et al., 2014), and [^{3}H]neurotransmitter uptake by the dopamine, norepinephrine, and serotonin transporters (Eshleman et al., 1999; Eshleman et al., 2013) were conducted as we have previously described in detail. Methods used to examine drug effects on other receptor-mediated signal transduction pathways are described below.

α_1-Adr -mediated Inositol-1-phosphate (IP-1) formation. HEK-α_{1A}-Adr, HEK-α_{1B}-Adr or HEK-α_{1D}-Adr cells were used for assays involving the IP-One Gq ELISA kit (CisBio, Bedford, MA). The methods are an adaptation of our 5HT2A IP-1 assay (Eshleman et al., 2013). The day before an experiment, cells were plated in 24 well plates at a density of 400,000 cells/well using DMEM supplemented with charcoal-stripped FetalClone and penicillin/streptomycin. For HEK-α_{1A}-Adr cells, on the day of the experiment, medium was removed, and cells were pre-incubated with 1 ml unsupplemented medium for 1 hr. HEK-α_{1B}-Adr or HEK-α_{1D}-Adr cells were used without rinsing. Drugs were made up in stimulation buffer supplied in the kit supplemented with 100 µM tropolone. Medium was removed from the well, antagonist or buffer was added, and cells were preincubated for 10 min. Agonists were added and cells were incubated for 1 hour, lysed for 30 min, and 50 µl of cell lysate was added to the IP-1 plates. After the addition of

JPET Fast Forward. Published on June 8, 2020 as DOI: 10.1124/jpet.120.265561
This article has not been copyedited and formatted. The final version may differ from this version.

appropriate antibodies, plates were incubated overnight at 4°C, washed 6 times, incubated with substrate for 20 min, and after termination of the reaction, the plate was read on a plate reader at 450 nm with a correction at 620 nm. Agonist effects were normalized to the maximal stimulation by norepinephrine, and antagonists were tested in the presence of 100 nM norepinephrine and normalized to the inhibition by 100 nM tamsulosin.

Opioid (delta and kappa) Receptor-mediated [^{35}S]GTPγS Binding: The membranes for [^{35}S]GTPγS binding assays were prepared in 20 mM HEPES, 10 mM $MgCl_2$, 100 mM NaCl and 0.2 mM DTT (pH 7.4). Cells were scraped from the plates and centrifuged at 500 x g for 15 min. The resulting pellet was homogenized in 2 ml buffer with a polytron, diluted with 11 ml buffer, and centrifuged at 40,000 x g for 15 min, washed and recentrifuged. The final pellet was covered with 3 ml buffer and stored at -80°C until needed. The membranes were incubated with [^{35}S]GTPγS (50 pM), GDP (10 μM), and the test compound, in a total volume of 1 ml, for 60 min at 25°C (Traynor and Nahorski, 1995). Samples were filtered over Perkin Elmer FiltermatA filters and counted as described for the binding assays. A dose response curve with a prototypical full agonist (DPDPE, and U69,593 for DORs and KORs, respectively) was conducted in each experiment to identify full and partial agonists.

Opioid (mu) Receptor-mediated [^{35}S]GTPγS Binding Comparisons of morphine-like and synthetic opioids on β-arrestin 2 have been well described (de Waal et al., 2020; Vasudevan et al., 2020). Fentanyl and related analogues, as well as morphine-like compounds exert effects via a β-arrestin 2-mediated pathway that is hypothesized to play a role in the unwanted side-effects of opioids. Here we executed a head-to-head comparison of the effects of morphine and fentanyl on opioid receptor-mediated $G\alpha_{i/o}$ activation as well as effects on non-opioid receptor function. Membranes were prepared in 20 mM HEPES, 10 mM $MgCl_2$, 100 mM NaCl, 1 mM EDTA and 0.2 mM DTT (pH 7.4). Cells were starved for 12-18 hr prior to harvest in unsupplemented DMEM. Cells were scraped from the plates and centrifuged at 500 x g for 15

min. The cell pellet was homogenized in 2 ml buffer with a polytron, diluted with 11 ml buffer, and centrifuged at 40,000 x g for 15 min, washed and recentrifuged. The final pellet was overlaid with 3 ml of buffer and stored at -80^{o}C until use. For agonist assays, the membrane was incubated with [^{35}S]GTPγS (50 pM), GDP (1 μM), and the test compound, in a total volume of 1 mL, for 60 min at 25˚C. Samples were filtered over glass fiber filters and washed with ice cold saline. A dose response curve with DAMGO was conducted in each agonist experiment to identify full and partial agonist compounds.

Data analysis

Sigmoidal curves resulting in IC_{50} values for displacement of radioligand or inhibition of second messenger generation were analyzed using a non-linear curve-fitting program and further analyzed using unpaired t-tests or one-way ANOVAs followed by either Dunnett's or Tukey's multiple comparisons test (Prism version 7, GraphPad Software, La Jolla, CA). Saturation binding data were analyzed by non-linear regression to generate K_D and B_{max} values as we have previously described (Eshleman et al., 2013; Janowsky et al., 2014; Eshleman et al., 2018).

Results

Fentanyl and morphine interactions with opioid receptor subtypes.

Fentanyl and morphine **(Figure 1)** had highest affinity for MOR ([^{3}H]DAMGO binding), as compared to their affinities for KOR and DOR subtypes, and the rank order of affinities across receptors were similar (mu>>kappa>delta) (Table 1). However, fentanyl had higher selectivity, i.e., its affinities for KOR (357 fold) and DOR (697 fold) were much lower than its affinity for the MOR, as compared to morphine, which differed less in affinities for the KORs (46 fold) and DORs (306 fold). In assays of receptor function ([^{35}S]GTPγS binding), potency differences paralleled affinity differences in terms of selectivity. Fentanyl was an apparent full agonist at the

JPET Fast Forward. Published on June 8, 2020 as DOI: 10.1124/jpet.120.265561
This article has not been copyedited and formatted. The final version may differ from this version.

MOR, but under the assay conditions described here, was a partial agonist at DOR (71% efficacy compared to DPDPE, $p<0.0001$, one-way ANOVA followed by Dunnett's multiple comparison test) and KOR (85% compared to U50,488H, $p<0.05$). Morphine, however, was a full agonist at KOR but a partial agonist at DOR ($p<0.05$) and MOR ($p<0.01$). (Table 1).

Fentanyl, carfentanil, morphine and naloxone interactions with α_1-Adr subtypes.

In initial experiments, equilibrium saturation binding of [^{3}H]prazosin to recombinant human α_{1A}-Adr, α_{1B}-Adr, and α_{1D}-Adr subtypes stably expressed in HEK293 cells was characterized and Kd and Bmax values were determined (Table 2). For α_{1A}-Adr, the [^{3}H]prazosin Kd was 0.153 ± 0.052 nM and the Bmax was 6.39 ± 0.3 pmol/mg protein. For α_{1B}-Adr, the Kd was 0.147 ± 0.018 nM and the Bmax was 7.7 ± 1.7 pmol/mg protein. For α_{1D}-Adr, the Kd was 0.186 ± 0.003 nM and the Bmax was 1.12 ± 0.18 pmol/mg protein. Thus, the Kd values across receptor subtypes were in the high picomolar range, but differed significantly (one-way ANOVA followed by Tukey's multiple comparison test, $p<0.05$). These Kd values were used to calculate Ki values in subsequent experiments that examined drug-receptor interactions (Cheng and Prusoff, 1973).

Fentanyl had Ki values in the low micromolar range at each receptor subtype, with a rank order of affinity of α_{1B}-Adr≥α_{1A}-Adr>α_{1D}-Adr ($p<0.001$, one way ANOVA followed by Tukey's multiple comparison, Table 3, Figure 2). Carfentanil similarly demonstrated Ki values in the low micromolar range with a rank order of affinity of α_{1A}-Adr>α_{1B}-Adr>α_{1D}-Adr. In contrast, Ki values for morphine and naloxone at each receptor subtype were greater than 100 µM. Norepinephrine, epinephrine, and phenylephrine displaced [^{3}H]prazosin binding with rank orders of affinity of α_{1D}-Adr>>α_{1A}-Adr≥α_{1B}-Adr (Table 3, $p<0.01$, one way ANOVA followed by Tukey's multiple comparison). Importantly, fentanyl and norepinephrine, the endogenous agonist, had similar affinities for α_{1A}-Adr and α_{1B}-Adr ($p>0.05$, one way ANOVA followed by Dunnett's multiple comparison), whereas carfentanil had a ~3 fold higher affinity at α_{1A}-Adr. Carfentanil had higher

JPET Fast Forward. Published on June 8, 2020 as DOI: 10.1124/jpet.120.265561
This article has not been copyedited and formatted. The final version may differ from this version.

affinity than norepinephrine at α_{1B}-Adr, but both fentanyl and carfentanil had much lower affinity than norepinephrine at α_{1D}-Adr (Table 3, $p<0.0001$), where norepinephrine had its greatest affinity by ~10-20 fold over α_{1A}-Adr and α_{1B}-Adr, respectively. The competitive binding pattern of F/FAs suggested by the compounds tested, if consistent among members of this class of drugs/opioids, may allow for the increased availability and coalescence of NE at α_{1D}-Adr and offers an explanation for the consistency of the clinical effects seen with F/FAs. These differences in affinities and availability of NE for α_{1D}-Adr binding could play an important role in the effects of F/FAs on noradrenergic system function in the LC (primary noradrenergic system in mammalian CNS) and cardiovascular system, given the key distribution and variations in subtype dominance of α_1-AdRs in these anatomic locations.

Epinephrine had higher affinity for α_{1D}-Adr than does fentanyl ($p<0.001$) and similar affinities as fentanyl at α_{1A}-Adr and α_{1B}-Adr ($p>0.05$). Phenylephrine had much lower affinity at α_{1A}-Adr and α_{1B}-Adr (ps<0.01) but similar affinity at α_{1D}-Adr than fentanyl ($p>0.05$), and these differences in affinity could affect response to agonist when fentanyl is present. It is noteworthy that carfentanil had greater affinity at the α_{1A}-Adr than epinephrine by nearly two fold. Prazosin and tamsulosin, receptor antagonists, had much higher affinity for [^{3}H]prazosin binding at each receptor subtype than did fentanyl or carfentanil (ps<0.001) and the Adr agonists (Table 3). However, prazosin had similar affinities for the subtypes, while tamsulosin affinities at the subtypes varied (α_{1A}-Adr≥α_{1D}-Adr>>α_{1B}-Adr, $p<0.01$), suggesting that each might be a useful tool for altering noradrenergic function affected by fentanyl, carfentanil or other F/FAs.

In assays of receptor function, neither morphine, fentanyl nor carfentanil had agonist activity at any α_1-Adr subtype (Table 3, Figure 3). The morphine IC_{50} value at blocking norepinephrine-stimulated IP-1 accumulation was greater than 100 μM at each receptor subtype. Conversely, fentanyl was a relatively weak antagonist at α_{1D}-Adr, and inhibited 73% of norepinephrine-mediated IP-1 accumulation. At α_{1A}-Adr and α_{1B}-Adr, fentanyl blocked 100% of

JPET Fast Forward. Published on June 8, 2020 as DOI: 10.1124/jpet.120.265561
This article has not been copyedited and formatted. The final version may differ from this version.

norepinephrine-stimulated IP-1 accumulation and had higher potency, as compared to effects at α_{1D}-Adr (Table 3, $p<0.01$). Similarly, carfentanil was an antagonist with rank order of potency α_{1B}-Adr > α_{1A}-Adr > α_{1D}-Adr. Norepinephrine and epinephrine had similar potencies ($ps>0.05$) and full efficacy at each α_1-Adr subtype, while phenylephrine had much lower potency than the neurotransmitters at each receptor subtype ($ps<0.001$), and was a partial agonist at α_{1D}-Adr. Prazosin and tamsulosin completely blocked norepinephrine-stimulated IP-1 accumulation, with the same rank order of potencies (α_{1D}-Adr>> α_{1A}-Adr= α_{1B}-Adr, $ps<0.05$) (Table 3).

Fentanyl and morphine interactions with the VMAT2 and neurotransmitter transporters.

Table 4 and Figure 4A, B, and C indicate that fentanyl and carfentanil were very weak at displacing [^{125}I]RTI-55 binding from the dopamine, serotonin and norepinephrine transporters, with Ki values ranging from >10 µM to 69 µM. Morphine's affinity for the binding site at each transporter was even lower, with Ki values at or above 75 µM. Consistent with previous reports, cocaine displaced radioligand binding from the dopamine, serotonin and norepinephrine transporters (Eshleman et al., 1999) with Ki values ranging from 404 to 1550 nM. Also consistent with previous reports, methamphetamine's Ki values ranged from 2.7 µM at the [^{125}I]RTI-55 binding site on the dopamine transporter to 117 µM at the serotonin transporter. At the VMAT2, fentanyl had a Ki value for displacing [^{3}H]DHTB of 56 µM, and the carfentanil and morphine Ki values were over 10 µM and 100 µM, respectively (Table 3, Figure 4D). Consistent with previous reports, methamphetamine, a VMAT2 substrate, was very weak at displacing [^{3}H]DHTB binding from the VMAT2, with a Ki value of 684 µM (Eshleman et al., 2013). DHTB, included as a control for the assay, had a Ki of 74 nM.

Because drugs differ between their affinities for radioligand binding sites on transporters and their potencies at inhibiting transporter function, we examined [^{3}H]neurotransmitter uptake by the respective recombinant human transporters and hVMAT2. The data in Table 4 and

JPET Fast Forward. Published on June 8, 2020 as DOI: 10.1124/jpet.120.265561
This article has not been copyedited and formatted. The final version may differ from this version.

Figure 5 indicate that IC_{50} values for morphine were greater than 100 µM, except at the serotonin transporter (>83 µM). Fentanyl, however, had IC_{50} values ranging from 27.5 µM at the norepinephrine transporter and 29.7 µM at the dopamine transporter, to >85 µM at the serotonin transporter. Carfentanil had an IC_{50} value of 4.46 µM at the norepinephrine transporter. Importantly, and in contrast to morphine (IC_{50} > 100 µM), the fentanyl IC_{50} value for blocking [^{3}H]5-HT uptake by the hVMAT2 was 911nM (Figure 5D), which is more potent than methamphetamine at blocking uptake (4 µM, p<0.0001, one way ANOVA Dunnett's multiple comparisons) (Table 4). The Ki/IC_{50} ratio suggests that both fentanyl (ratio 61) and methamphetamine (ratio 164) are binding to a site on the hVMAT2 that is more closely related to transporter function than is the [^{3}H]DHTB binding site (ratio 1.8) (Provencher et al., 2018). Carfentanil had an IC_{50} value of 4.1 µM at the VMAT2.

Fentanyl and morphine interactions with dopamine receptor subtypes.

The data in Table 5 and Figure 6 indicate that morphine, at concentrations up to 100 µM, did not displace radioligand binding from any dopamine receptor subtype. Fentanyl, however, had Ki values of ~1 µM and ~1.7 µM at the dopamine D4.4 [^{3}H]spiperone binding site and the dopamine D1 [^{3}H]SCH 23390 binding site, respectively. At the [^{3}H]spiperone binding sites on other D2-like receptors, fentanyl's Ki values were ~15 µM (D2) and ~12 µM (D3), indicating selectivity for the D4.4 receptor (Table 5, Figure 6D). Dopamine receptor agonists (SKF38393, quinpirole) and antagonists (SCH 23390, butaclamol, haloperidol) had Ki values for radioligand displacement resembling previously reported concentrations (Janowsky et al., 2014).

To determine if fentanyl or morphine affects dopamine D1 or D4.4 function, we examined their ability to modulate adenylyl cyclase activity that is stimulated (D1) or blocked (D4.4) by these receptors, respectively. Table 6 and Figure 7A indicate that neither fentanyl nor morphine stimulated adenylyl cyclase activity in C6-D1 cells. However fentanyl (but not

JPET Fast Forward. Published on June 8, 2020 as DOI: 10.1124/jpet.120.265561
This article has not been copyedited and formatted. The final version may differ from this version.

morphine) partially (65.5%) inhibited the activity elicited by 100 nM dihydrexidine with an IC_{50} value of 27 µM, while SCH 23390 completely blocked activation with an IC_{50} value of 3.9 nM (Figure 7B). In HEK-D4.4 cells, neither fentanyl nor morphine had agonist activity as measured by inhibition of forskolin-stimulated adenylyl cyclase activity (Figure 7C). Fentanyl, not morphine, was a D4.4 antagonist, partially (63%) blocking the quinpirole effect, with an IC_{50} value of 12.7 µM. Haloperidol completely blocked the quinpirole effect, with an IC_{50} value of 152 nM (Table 6, Figure 7D).

Fentanyl and morphine interactions with serotonin receptor subtypes.

Table 7 and Figure 8 indicate the affinities of fentanyl and morphine at the [^{3}H]8-OH-DPAT binding site on the recombinant h5-HT1A receptor and at [^{3}H]5-HT binding sites on the recombinant h5-HT2A, 2B, and 2C receptors. In all cases, morphine Ki values were over 100 µM. However, fentanyl Ki values ranged from ~2.2 µM at the 5-HT1A receptor to 114 µM at the 5-HT2C receptor. Other drugs, selective for the respective receptor subtypes, had effects resembling previously reported Ki values (Eshleman et al., 2013).

Fentanyl and morphine interactions with the recombinant human CB1 cannabinoid and NMDA (G2a/G1) receptors.

Table 7 indicates that neither fentanyl nor morphine displaced [^{3}H]CP 55,940 binding to the recombinant hCB1 cannabinoid receptor (Ki > 100 µM) or [^{3}H]MK-801 binding to the recombinant hNMDA (G2a/G1) receptor. Selective agents included in the assays for comparison had Ki values resembling previously reported values (Bresink et al., 1995; Pertwee, 2008b; Pertwee, 2008a).

Discussion

The hypothesis that deaths due to exposure from F/FAs are not mediated by MORs includes: 1) Naloxone availability has not significantly reduced F/FA-related deaths (Baumann et

JPET Fast Forward. Published on June 8, 2020 as DOI: 10.1124/jpet.120.265561
This article has not been copyedited and formatted. The final version may differ from this version.

al., 2018); 2) Fentanyl metabolites are almost non-existent in tissue from patients who died of fentanyl overdose, suggesting rapid cardiopulmonary collapse that contrasts with the effects of heroin (Burns et al., 2016); 3) Public health data from death scenes and eyewitness reports of F/FA-related deaths show consistent evidence of rapid and atypical death compared with heroin overdose (Somerville et al., 2017); 4) Published data on drug effects in animal models, and radioligand binding data indicate that fentanyl causes the rapid onset of severe muscle rigidity *via* cerulospinal fibers innervated/controlled by α_1-Adr postsynaptic receptors (Lui et al., 1989; Tsou et al., 1989; Lui et al., 1990; Fu et al., 1997); 5) The principal effect of high-dose F/FAs is rapid closure of vocal cords followed by rigidity of the chest wall (Scamman, 1983; Bennett et al., 1997); 6) Fentanyl isolates the vagal medullary fibers that innervate the vocal cords contributing to vocal cord closure (Lalley, 2003a); 7) Activation of α_1-Adr subtypes facilitates excitatory inputs to medullary airway vagal preganglionic neurons that modulate laryngeal and tracheal musculature (Haxhiu et al., 2003; Ge et al., 2015).

Experimental results herein, comparing the effects of morphine, naloxone, norepinephrine, fentanyl and carfentanil in the same assay, indicated that pharmacologies differ, that fentanyl binds to α_1-Adrs, add new data on carfentanil-α_1-Adr subtype binding, and indicate the similar selectivity of fentanyl analogues to α_1-Adr subtypes as a possible underlying mechanism in the lethality of this synthetic opioid family. α_1-Adr subtypes have differing anatomical distributions that further implicates their role in the effects of fentanyl but not morphine. For example, the α_{1D}-Adr, but not α_{1A}-Adr or α_{1B}-Adr subtypes, found predominantly in the large coronary arteries, mediates vasoconstriction (Jensen et al., 2009). The α_{1B}-Adr, found in pulmonary arteries, mediates contraction (Sohn et al., 2005). Norepinephrine had the highest affinity for α_{1D}-Adr compared to α_{1A}-Adr and α_{1B}-Adr (Table 3). A large and rapid fentanyl-induced norepinephrine release (Hicks et al., 1981) should cause α_{1D}-Adr-mediated contraction of coronary arteries, negatively impacting cardiovascular function (Ray et al., 2016).

JPET Fast Forward. Published on June 8, 2020 as DOI: 10.1124/jpet.120.265561
This article has not been copyedited and formatted. The final version may differ from this version.

Interestingly, fentanyl was a very weak antagonist at α_{1D}-Adr, as compared to its ability to antagonize norepinephrine-mediated IP-1 formation at α_{1A}-Adr and α_{1B}-Adr (Table 3), suggesting a possible focusing of norepinephrine effects on the α_{1D}-Adr subtype when fentanyl is present.

Additionally fentanyl and carfentanil (but not morphine) blocked VMAT2-mediated neurotransmitter uptake (IC_{50} ~ 911 nM), but was much weaker at blocking radioligand binding (Table 4). Lobeline, a VMAT2 uptake blocker, has some structural similarities to fentanyl, and fentanyl is more potent than lobeline at blocking VMAT2-mediated [^{3}H]neurotransmitter uptake (lobeline IC_{50} = 4.2μM) (Provencher et al., 2018). Differing IC_{50} values for uptake and Ki values for binding are consistent with the effects of transporter substrates (Cozzi et al., 2009). The VMAT2 transports neurotransmitter into synaptic vesicles (Erickson et al., 1996), however, preliminary data indicated that the VMAT2 did not transport [^{3}H]fentanyl (data not shown). Thus, fentanyl appears to block uptake by, but not to displace neurotransmitter from the transporter/vesicle. The resulting increase in intracellular norepinephrine availability, and norepinephrine synaptic release via the presynaptic transporter, coupled with fentanyl blockade of α_{1A}- and α_{1B}-Adr (the α_{1D}-Adr has relatively lower affinity for fentanyl), could result in more selective α_{1D}-Adr stimulation, consistent with deleterious α_{1D}-mediated consequences including coronary artery vasospasm, as mentioned above.

Dopamine receptors had differential affinity for fentanyl, with the D1 and D4.4 receptors having the highest affinity, ~1 μM (Table 5), and fentanyl was a weak antagonist at both receptors (Table 6). In agreement with previous reports, fentanyl's potency at blocking D1 receptor-mediated cAMP accumulation (Govoni et al., 1975) was similar to fentanyl's affinity at blocking [^{3}H]SCH 23390 binding to the D1 receptor. Lalley (Lalley, 2005a; Lalley, 2005b) suggested that dopamine D1 receptor agonists might reverse opioid-induced respiratory depression but not antinociception, while antagonists enhance respiratory depression.

Therefore, fentanyl-mediated blockade of the D1 receptor subtypes should increase MOR-mediated respiratory depression, necessitating increased administration of naloxone, consistent with findings related to fentanyl overdose.

Previous reports also used [^{3}H]8-OH-DPAT to characterize fentanyl's effects at 5HT1A receptors, and obtained almost identical results (Ki ~2μM) (Rickli et al., 2018). However, we report that fentanyl had micromolar affinity (31μM) at the 5HT2A receptor as measured using an agonist, [^{3}H]5-HT, while Rickli and coworkers obtained a Ki value of 1.3μM using the antagonist [^{3}H]ketanserin. Differences in affinity for the binding sites could be due to the use of agonist versus antagonist ligand. We found no reports indicating direct effects of fentanyl on receptor function that could corroborate any differences in affinity caused by differences in radioligand. Fentanyl had very low affinity for the 5HT2C receptor, regardless of radioligand, and our data (Table 7) are the first indication of low affinity of fentanyl at the recombinant human 5HT2B receptor.

In agreement with a previous report (Fernandez-Fernandez et al., 2014) indicating that fentanyl did not displace [^{3}H]CP55,940 binding from CB1 receptors in human cortical preparations, neither fentanyl nor morphine displaced [^{3}H]CP55,940 binding from the recombinant human receptor (Table 7). Additionally, neither fentanyl nor morphine blocked [^{3}H]MK-801 binding to recombinant NMDA receptors (G2a/G1), in agreement with a report describing a rat cortical wedge preparation (Ebert et al., 1998). The low affinity precluded functional tests but both fentanyl and morphine, at high micromolar concentrations block the function of NMDA channels of various subunit composition expressed in *Xenopus* oocytes (Yamakura et al., 1999).

Whether the Ki and IC_{50} values described above are relevant to the symptoms of fentanyl overdose depend on pharmacokinetic assumptions. Fentanyl is lipophilic, and calculated brain lipid concentrations can reach almost 3 mM (Stone and DiFazio, 1988). The

high octanol:water partition coefficient for fentanyl (9,550) and carfentanil (~>13,000), suggests that toxic brain interstitial concentrations in the high nM - low μM range are relevant (Stone and DiFazio, 1988). However, calculations based on plasma drug concentrations suggest that brain concentrations are much lower (Kalvass et al., 2007; Heiskanen et al., 2015). Sheep models have demonstrated significant first pass peak concentrations reaching the brain after intravenous drug administration that may be up to 4,000 times greater than plasma concentrations within the first min of circulation (Upton, 1996). The pharmacokinetic assumptions, that illicit fentanyl administration results in very high (mM) concentrations in various compartments, suggests that our data (low μM Ki and IC_{50} values) at various receptors and transporters are pharmacologically relevant and contribute to the differences between morphine and fentanyl in clinical symptoms and outcomes.

The relevance of these findings is significant given the incidence of deaths from F/FAs. High doses of F/FAs in animal models increase signal output from the LC causing severe and sustained chest wall rigidity, and are mediated by the direct interaction of noradrenaline and α_1-Adr receptors (Lui et al., 1989). Similarly, LC output controls medullary vagal motor fibers innervating the airway, while fentanyl selectively activates vagal motor fibers (Haxhiu et al., 2003; Lalley, 2003b). These reports and our data support plausible mechanisms for increased noradrenergic activity and selective non-MOR receptor/VMAT2 transporter blockade that is the pre-requisite for synthetic opioid-induced overdose, with resulting laryngospasm, cardiovascular and secondary hepatic compromise (Yasuda et al., 1978; Scamman, 1983; Lui et al., 1989; Lui et al., 1990; Lui et al., 1993; Lui et al., 1995; Bennett et al., 1997; Burns et al., 2016; Somerville et al., 2017; Torralva and Janowsky, 2019). These mechanisms appear to be distinct from the effects of F/FA at MORs. (Sokoll et al., 1972).

F/FAs increase norepinephrine in peripheral circulation (Thomson et al., 1988). However, F/FAs, in fact all opioids, decrease norepinephrine release in the CNS (Aghajanian, 1982). Our new data demonstrate two mechanisms by which fentanyl may alter norepinephrine disposition: 1) fentanyl blocked intracellular vesicular reuptake of neurotransmitter (Figure 5), increasing their cytoplasmic concentrations and 2) fentanyl selectively blocked α_1-Adr receptor subtypes (Table 3) in a manner that isolates and focuses noradrenergic activity on the α_{1D}-Adr subtype (Figure 3) where norepinephrine has its highest affinity.

Our hypothesis concerning a non-opioid fentanyl-modulated pathway has relevance for the current fentanyl-driven opioid crisis where the increased deaths and reduced sensitivity to naloxone may be due to acute vocal cord closure and cardiovascular dysfunction mediated by noradrenergic activity at α_{1D}-Adr receptors, where opioid antagonists would have little effect (Willette and Sapru, 1982; Torralva and Janowsky, 2019). These data suggest the underlying mechanisms for FIRE and indicate new directions for development of supplementary modes of emergency treatment and strategic interventional targets (e.g. α_1-Adr receptor subtypes) that may improve survival from F/FA exposure.

In conclusion, the current novel data may be relevant to the development of therapeutics targeting the underlying mechanism of the adverse effects and deaths associated with F/FAs. The affinity and effects of fentanyl at α_1-Adr subtypes and the VMAT2 differ significantly from morphine. Thus, profiling of new fentanyl analogues and synthetic opioids against the receptor panel described here could help to identify therapeutic candidates with fewer adverse clinical effects and indicate strategic intervention points for the lethal mechanisms of these compounds.

Acknowledgements

The contents do not represent the views of the U.S. Department of Veterans Affairs or the United States Government.

Authorship Contributions:

Participated in research design: Torralva, Eshleman, Schutzer, Janowsky

Conducted experiments: Eshleman, Swanson, Schmachtenberg, Bloom, Wolfrum, Reed

Performed data analysis: Swanson, Schmachtenberg, Bloom, Wolfrum, Reed, Schutzer, Eshleman, Janowsky

Wrote or contributed to the writing of the manuscript: Torralva, Eshleman, Schutzer, Swanson, Schmachtenberg, Bloom, Wolfrum, Reed, Janowsky

Footnotes:

Funding Funding for this study was provided by the United States Department of Justice, Drug Enforcement Administration [D-15-OD-0002], Department of Veterans Affairs Merit Review [I01BX002758] and Career Scientist programs [14S-RCS-006], the National Institutes of Health/National Institute on Drug Abuse Methamphetamine Abuse Research Center [P50 DA018165], and a National Institutes of Health/National Institute on Drug Abuse interagency agreement [ADA12013]. The contents do not represent the views of the U.S. Department of Veterans Affairs, U.S. Department of Justice, Drug Enforcement Administration or the United States Government.

Conflict of interest

All authors declare that they have no conflicts of interest.

Figure 1. Structures of morphine, fentanyl and carfentanil.

Figure 2. Displacement of specific [^{3}H]Prazosin binding by opioids and antagonists at (A) α_{1A}-Adr, (B) α_{1B}-Adr, and (C) α_{1D}-Adr receptor subtypes. Data shown are the mean ± sem of 3-5 experiments, except if a drug had no effect when n=2.

Figure 3: HEK-α_{1A}-Adr, HEK-α_{1B}-Adr, and HEK-α_{1D}-Adr: IP-1 agonist and antagonist dose-response curves. A, B, C: agonist stimulation of IP-1 formation: A, α_{1A}-Adr; B, α_{1B}-Adr 1B; C, α_{1D}-Adr receptor subtypes. D, E, F: antagonist inhibition of norepinephrine-stimulated IP-1 formation. D, α_{1A}-Adr; E, α_{1B}-Adr; F, α_{1D}-Adr receptor subtypes. Data shown are the mean ± sem of 3-6 experiments, except if a drug had no effect when n=2.

Figure 4: Opioid effects on radioligand binding to transporters. A, ([^{125}I]RTI-55) binding to HEK-hDAT; B, to -hSERT; C, to –hNET; and D, [^{3}H]DHTB binding to -hVMAT2. Data shown are the mean ± sem of 3-5 experiments, except if a drug had no effect when n=2.

Figure 5: Opioid effects on [^{3}H]neurotransmitter uptake by HEK-hDAT, -hSERT, -hNET, and -hVMAT2. A, hDAT ([^{3}H] DA); B, hSERT ([^{3}H] 5-HT); C, hNET ([^{3}H] NE); D, hVMAT2. ([^{3}H] 5-HT). Data shown are the mean ± sem of 3-5 experiments, except if a drug had no effect when n=2.

Figure 6: Drug effects on radioligand binding to dopamine D1, D2, D3 and D4.4 receptors. A, dopamine D1 receptor ([^{3}H]SCH 23390); B, dopamine D2 receptor ([^{3}H]spiperone); C, dopamine D3 receptor ([^{3}H]spiperone); D, dopamine D4.4 receptor ([^{3}H]spiperone). Data shown are the mean ± sem of 3-7 experiments.

Figure 7. Agonist, antagonist, and opioid effects on dopamine D1 and D4.4 receptor-mediated adenylyl cyclase. A, D1 agonist stimulation of adenylyl cyclase; B, D1 antagonist inhibition of 100 nM dihydrexidine-stimulated adenylyl cyclase activity; C, D4.4 agonist inhibition of 10 µM

forskolin-stimulated adenylyl cyclase; D, D4.4 antagonist reversal of 2 nM quinpirole inhibition of forskolin-stimulated adenylyl cyclase. Data shown are the mean ± sem of 3-6 experiments.

Figure 8: Drug effects on radioligand binding to serotonin 5HT1A, 5HT2A, 5HT2B and 5HT2C receptors. A, 5HT1A receptor ([^{3}H]8-OH-DPAT); B, 5HT2A receptor ([^{3}H]5-HT); C, 5HT2B receptor ([^{3}H]5-HT); D, 5HT2C receptor ([^{3}H]5-HT). Data shown are the mean ± sem of 3-7 experiments.

JPET Fast Forward. Published on June 8, 2020 as DOI: 10.1124/jpet.120.265561
This article has not been copyedited and formatted. The final version may differ from this version.

Table 1. Fentanyl and Morphine Interactions with Opioid Receptor Subtypes

	CHO-rMOR [^{3}H]DAMGO Binding	CHO-hKOR [^{3}H]U69,593 Binding	CHO-hDOR [^{3}H]DPDPE Binding
Drug	Ki (nM) ± sem (n)	Ki (nM) ± sem (n)	Ki (nM) ± sem (n)
	Hill slope ± sem	Hill slope ± sem	Hill slope ± sem
Fentanyl	0.35 ± .05 (16)	125 ± 15 (14)	244 ± 20 (12)
	-0.78 ± 0.05	-0.95 ± 0.05	-1.07 ± 0.04
Morphine	0.58 ± 0.8 (19)	27 ± 3 (15)	178 ± 14 (12)
	-0.97 ± 0.05	-0.98 ± 0.04	-1.06 ± 0.04
	[^{35}S]GTPɣS Binding	[^{35}S]GTPɣS Binding	[^{35}S]GTPɣS Binding
	EC_{50} (nM) ± sem (n)	EC_{50} (nM) ± sem (n)	EC_{50} (nM) ± sem (n)
	% max DAMGO Stimulation ± sem	% max U69,593 Stimulation ± sem	% max DPDPE Stimulation ± sem
Fentanyl	18 ± 4 (12)	389 ± 41 (14)	1256 ± 153 (13)
	92 ± 4%	85 ± 5%	71 ± 5%
Morphine	38 ± 6 (13)	47 ± 6 (12)	789 ± 92 (13)
	86 ± 3%	94 ± 4%	89 ± 4%

Experiments were conducted as described in the text. (n) = number of independent experiments, each conducted with duplicate determinations.

Table 2: [^{3}H]Prazosin saturation binding to HEK-α_{1A}-Adr, HEK- α_{1B}-Adr, and HEK-α_{1D}-Adr receptor subtypes: [^{3}H]Prazosin Kd and Bmax values

Receptor	[^{3}H]Prazosin Binding	
	Bmax (pmol/mg) ± sem (n)	Kd (nM) ± sem
α_{1A}-Adr	6.39 ± 0.30 (3)	0.153 ± 0.052
α_{1B}-Adr	7.7 ± 1.7 (3)	0.147 ± 0.018
α_{1D}-Adr	1.12 ± 0.18 (3)	0.186 ± 0.003

[^{3}H]Prazosin was tested at concentrations ranging from 0.08-2.5 nM. Assays were conducted in duplicate. Experiments were conducted as described in the text. (n) = number of independent experiments, each conducted with duplicate determinations.

Table 3: HEK-α_{1A}-Adr, HEK- α_{1B}-Adr, and HEK- α_{1D}-Adr: Effects of fentanyl, carfentanil, morphine, naloxone and Adr 1 agonists and antagonists on [^{3}H]prazosin binding and IP-1 formation.

Drug	[^{3}H]Prazosin Binding Ki (nM) ± sem (n) Hill slope ± sem			Drug-Stimulated IP-1 Accumulation EC_{50} (nM) ± sem (n) % max NE ± sem[a]			Inhibition of NE-stimulated IP-1 Accumulation IC_{50} (nM) ± sem (n) % max inhibition ± sem[b]		
	α_{1A}-Adr	α_{1B}-Adr	α_{1D}-Adr	α_{1A}-Adr	α_{1B}-Adr	Adr1D	α_{1A}-Adr	α_{1B}-Adr	α_{1D}-Adr
Fentanyl	1407 ± 81 (5) -1.32 ± 0.05	1100 ± 250 (3) -1.51 ± 0.08	4110 ± 450 (4) -1.41 ± 0.21	>100 µM (2) 0%	>100 µM (2) <1%	>20 µM (6) 3.5 ± 2.5%	3660 ± 790 (3) 100%	3690 ± 300 (3) 100%	11,900 ± 1,600 (3) 73 ± 13%
Carfentanil	418 ± 24 -1.35 ± 0.04	828 ± 57 -1.93 ± 0.31	2490 ± 530 -1.54 ± 0.11	>10 µM (5) 0%	>10 µM (2) 0%	>10 µM (2) 0%	2040 ± 380 (6) 100%	1030 ± 150 (6) 99.9 ± 0.1%	>10 µM (3) 5.7 ± 2.6%
Morphine	>100 µM (2) ND	>100 µM (2) ND	>100 µM (2) ND	>100 µM (2) 0%	>100 µM (2) <3%	>100 µM (4) 0%	>100 µM (2) 16.3 ± 3.7%	>100 µM (2) <7%	>100 µM (2) <5%
Naloxone	>100 µM (2) ND	>100 µM (2) ND	>100 µM (2) ND						
Norepinephrine	1580 ± 220 (5) -1.01 ± 0.04	1920 ± 490 (3) -1.45 ± 0.20	131 ± 40 (5) -0.94 ± 0.15	55 ± 12 (3) 102.8 ± 3.3%	39.7 ± 5.8 (3) 104.1 ± 3.6%	37.0 ± 5.8 (3) 95.89 ± 0.63%			
Epinephrine	730 ± 140 (3)	790 ± 150 (3)	185 ± 22 (3)	22.7 ± 5.0 (4)	10.0 ± 2.3 (3)	32.1 ± 9.8 (3)			

	-1.05 ± 0.07	-1.23 ± 0.05	-1.06 ± 0.03	106.1 ± 1.4%	100.6 ± 4.7%	103.0 ± 4.6%			
Phenylephrine	4880 ± 410 (5)	4900 ± 1100 (3)	1850 ± 230 (3)	318 ± 13 (3)	330 ± 110 (4)	620 ± 140 (4)			
	-1.26 ± 0.09	-1.92 ± 0.39	-1.11 ± 0.05	106.3 ± 1.6%	95.3 ± 5.9%	70.1 ± 1.2%			
Prazosin	0.134 ± 0.057 (3)	0.027 ± 0.008 (3)	0.115 ± 0.037 (4)				4.02 ± 0.54 (3)	8.7 ± 2.7 (5)	0.48 ± 0.12 (3)
	-0.72 ± 0.09	-0.56 ± 0.04	-0.51 ± 0.09				100%	100%	99.06 ± 0.77%
Tamsulosin	0.038 ± 0.013 (3)	0.769 ± 0.043 (3)	0.084 ± 0.023 (3)				1.95 ± 0.85 (4)	5.04 ± 0.44 (4)	0.339 ± 0.061 (4)
	-0.96 ± 0.05	-1.05 ± 0.05	-0.56 ± 0.07				100%	100%	100%

For each receptor, standard agonists and antagonists were tested: Adr1 agonists NE, EPI and phenylephrine and Adr1 antagonists prazosin and tamulosin. (n) = number of independent experiments, each conducted with duplicate determinations.

[a]Maximal agonist effects were normalized to the maximal stimulation by 10 µM norepinephrine.

[b]Maximal antagonist effects were normalized to the maximal inhibition by 100 nM tamsulosin.

Table 4: Ki values for inhibition of radioligand binding to, and IC_{50} values for inhibition of [^{3}H]neurotransmitter uptake by HEK-hDAT, HEK-hSERT, HEK-hNET and HEK-hVMAT2 cells.

Drug	hDAT [^{125}I]RTI-55 binding Ki (nM) ± sem Hill slope ± sem (n)	hDAT [^{3}H]DA uptake IC_{50} (nM) ± sem (n)	hSERT [^{125}I]RTI-55 binding Ki (nM) ± sem Hill slope ± sem (n)	hSERT [^{3}H]5-HT uptake IC_{50} (nM) ± sem (n)	hNET [^{125}I]RTI-55 binding Ki (nM) ± sem Hill slope ± sem	hNET [^{3}H]NE uptake IC_{50} (nM) ± sem (n)	hVMAT2 [^{3}H]DHTB binding Ki (nM) ± sem Hill slope ± sem (n)	hVMAT [^{3}H]5-HT uptake IC_{50} (nM) ± sem (n)
Fentanyl	40,270 ± 2,400 -1.17 ± 0.19 (3)	29,700± 7,700 (4)	69,000 ± 15,000 -1.20 ± 0.06 (5)	>85,000 (3)	13,000 ± 2800 -1.42 ± 0.40 (3)	27,500 ± 6,700 (4)	56,100 ± 2,700 -1.48 ± 0.09 (3)	911 ± 34 (4)
Carfentanil	>10,000 (3)	>20,000 (4)	>10,000 (3)	>20,000 (3)	>10,000 (3)	4,460 ± 870 (3)	>10,000 (3)	4,100 ± 1,100 (3)
Morphine	>99 µM ND (3)	>100 µM (2)	>78 µM ND (3)	>83,000 (3)	>90,000 ND (5)	>100 µM (2)	>100 µM (3) ND	>100 µM (2)
Cocaine	554 ± 60 -1.12 ± 0.09 (4)	278 ± 32 (5)	404.4 ± 6.8 -1.06 ± 0.08 (3)	260 ± 100 (3)	1550 ± 250 -1.48 ± 0.30 (3)	303 ± 54 (5)		
METH	2,760 ± 660 -1.38 ± 0.04 (3)	62.6 ± 2.2 (3)	117,000 ± 14,000 -1.23 ± 0.16 (3)	5,800 ± 470 (3)	1630 ± 180 -1.12 ± 0.04 (5)	12.1 ± 1.2 (4)	684,000 ± 65,000 -1.01 ± 0.07 (3)	4,180 ± 600 (4)
DHTB							74 ± 28 -1.28 ± 0.13 (3)	41.5 ± 3.3 (5)

ND: Hill slope was not determined due to the low affinity of the compound. For each transporter, methamphetamine (METH) was tested as a standard substrate. For DAT, SERT and NET, cocaine was tested as the standard blocker. For VMAT2, DHTB was tested as the standard blocker. (n) = number of independent experiments, each conducted with duplicate determinations.

JPET Fast Forward. Published on June 8, 2020 as DOI: 10.1124/jpet.120.265561
This article has not been copyedited and formatted. The final version may differ from this version.

Table 5: Drug effects on radioligand binding to dopamine D1, D2, D3 and D4.4 receptors.

Drug	DA D1R [^{3}H]SCH 23390 Ki (nM) ± sem (n) Hill slope ± sem	DA D2R [^{3}H]Spiperone Ki (nM) ± sem (n) Hill slope ± sem	DA D3R [^{3}H]Spiperone Ki (nM) ± sem (n) Hill slope ± sem	DA D4.4R [^{3}H]Spiperone Ki (nM) ± sem (n) Hill slope ± sem
Fentanyl	1,670 ± 200 (3) -1.17 ± 0.07	14,900 ± 1,800 (3) -1.20 ± 0.06	12,100 ± 910 (5) -0.88 ± 0.11	1,049 ± 74 (3) -1.13 ± 0.02
Morphine	>100 µM (3) ND	>100 µM (3) ND	>100 µM (3) ND	>100 µM (3) ND
SKF38393	79 ± 12 (3) -1.03 ± 0.04			
SCH23390	0.159 ± 0.018 (3) -1.16 ± 0.03			
Quinpirole		15,700 ± 4,900 (6) -0.79 ± 0.08	130 ± 20 (6) -0.73 ± 0.03	157.4 ± 7.8 (3) -0.80 ± 0.01
Butaclamol		0.58 ± 0.13 (7) -0.83 ± 0.18	8.2 ± 3.5 (6) -1.15 ± 0.30	
Haloperidol				4.60 ± 0.27 (3) -0.98 ± 0.01

For each receptor, a standard agonist (SKF 38393 or quinpirole) and antagonist (SCH23390, butaclamol or haloperidol) was tested. (n) = number of independent experiments, each conducted with duplicate determinations.

Table 6. Effects of fentanyl and morphine on recombinant human dopamine D1 and D4.4 receptor function

Drug (Agonists)	C6-D1 EC_{50} (nM) ± sem (n) % max Dopamine ± sem	C6-D1 IC_{50} (nM) ± sem (n) % max inhibition of 100 nM Dihydrexidine ± sem	HEK-D4.4-AC1 EC_{50} (nM) ± sem (n) % max Quinpirole ± sem	HEK-D4.4-AC1 IC_{50} (nM) ± sem (n) % max reversal of 100 nM Quinpirole ± sem
Fentanyl	>100 µM (2) 0%	27,000 ± 5,500 (5) 65.5 ± 4.0%	>50 µM (6) (3 of 6 curves could be fit) 36 ± 11%	12,700 ± 2,500 (4) 63 ± 20%
Morphine	>100 µM (2) 13 ± 13%	>100 µM (2) 4.5 ± 4.5%	>40 µM (5) (3 of 5 curves could be fit) 20 ± 11%	>100 µM (3) Minimal effect
Dopamine	19.5 ± 1.7 91.6 ± 5.9%		4.4 ± 1.5 (4) 95.1 ± 1.8%	
Quinpirole			0.60 ± 0.25 (6) 95.4 ± 3.9%	
SCH 23390		3.90 ± 0.52 (4) 98.36 ± 0.26%		

Haloperidol	152 ± 55 (4) 117 ± 26%

Assays were run in duplicate with 6-7 concentrations of the test compound. The standard agonist dopamine was tested in the agonist experiments and the antagonists SCH23390 (D1) or haloperidol (D4.4) were tested in the antagonist experiment. (n) = number of independent experiments, each conducted with duplicate determinations.

Table 7: Displacement of [^{3}H]radioligand from recombinant human serotonin 5HT1A, 5HT2A, 5HT2B, 5HT2C, and cannabinoid CB1 and glutamate NMDA (G2a/G1) receptors.

Drug	5HT1A [^{3}H]8-OH-DPAT Binding Ki (nM) ± sem (n) Hill slope ± sem	5HT2A [^{3}H]5-HT Binding Ki (nM) ± sem (n) Hill slope ± sem	5HT2B [^{3}H]5-HT Binding Ki (nM) ± sem (n) Hill slope ± sem	5HT2C [^{3}H]5-HT Binding Ki (nM) ± sem (n) Hill slope ± sem	CB1 [^{3}H]CP,940 binding Ki (nM) ± sem (n) Hill slope ± sem	NMDA (G2a/G1) [^{3}H]MK-801 binding Ki (nM) ± sem Hill slope ± sem
Fentanyl	2240 ± 240 (3) -1.06 ± 0.03	31,400 ± 3,000 (3) -1.02 ± 0.03	8,600 ± 1,200 (3) -0.87 ± 0.09	114,000 ± 23,000 (3) -0.89 ± 0.02	>100 µM (2)	>52 µM (4)
Morphine	>100 µM (3) ND	>100 µM (3) ND	>100 µM (3) ND	>100 µM (3) ND	>100 µM (2)	>100 µM (2)
5-HT	5.89 ± 0.71 (3) -0.90 ± 0.06	26.77 ± 0.56 (3) -1.03 ± 0.10	3.24 ± 0.11 (3) -0.87 ± 0.03	6.46 ± 0.77 (3) -0.96 ± 0.03		

WAY 100635	0.60 ± 0.33 (7)					
	-1.27 ± 0.22					
Ketanserin		13.1 ± 1.3 (3)				
		-0.43 ± 0.04				
SB204741			52 ± 14 (3)			
			-0.63 ± 0.06			
SB242084				2.87 ± 0.67		
				-1.17 ± 0.16		
WIN 55,212					244 ± 78 (3)	
					-0.80 ± 0.06	
THC					30 ± 10 (5)	
					-0.82 ± 0.18	
MK-801						12.3 ± 1.6 (5)
						-0.80 ± 0.06
Phencyclidine						2,870 ± 420 (8)
						-1.03 ± 0.14

For each serotonin receptor subtype, the standard agonist 5-HTand a selective antagonist (WAY 100635, ketanserin, SB204741 or SB242084) were tested. For the CB1 receptor, the standard agonists WIN 55,212 and THC were tested. For the NMDA receptor, the

standard antagonists MK-801 and phencyclidine were tested. (n) = number of independent experiments, each conducted with duplicate determinations.

JPET Fast Forward. Published on June 8, 2020 as DOI: 10.1124/jpet.120.265561
This article has not been copyedited and formatted. The final version may differ from this version.

Figure 1. Structures of morphine, fentanyl and carfentanil

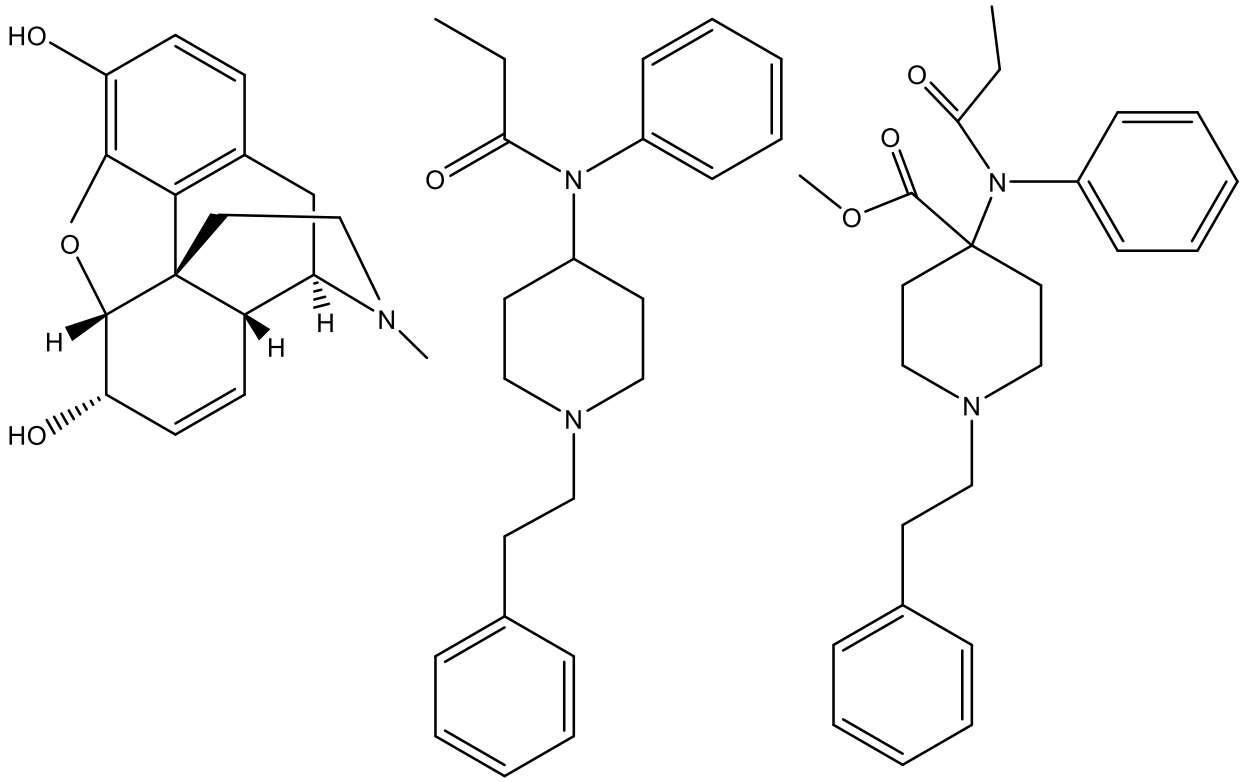

Morphine **Fentanyl** **Carfentanil**

JPET Fast Forward. Published on June 8, 2020 as DOI: 10.1124/jpet.120.265561
This article has not been copyedited and formatted. The final version may differ from this version.

Figure 2

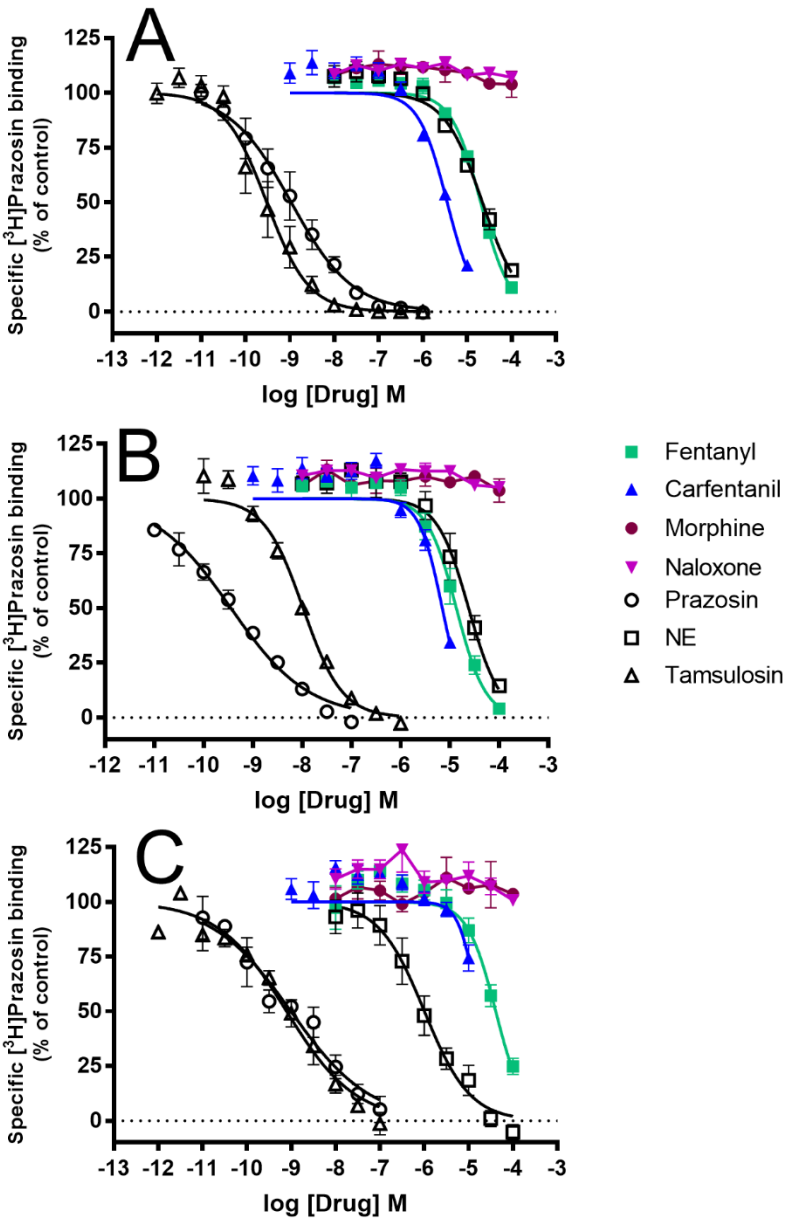

JPET Fast Forward. Published on June 8, 2020 as DOI: 10.1124/jpet.120.265561
This article has not been copyedited and formatted. The final version may differ from this version.

Figure 3

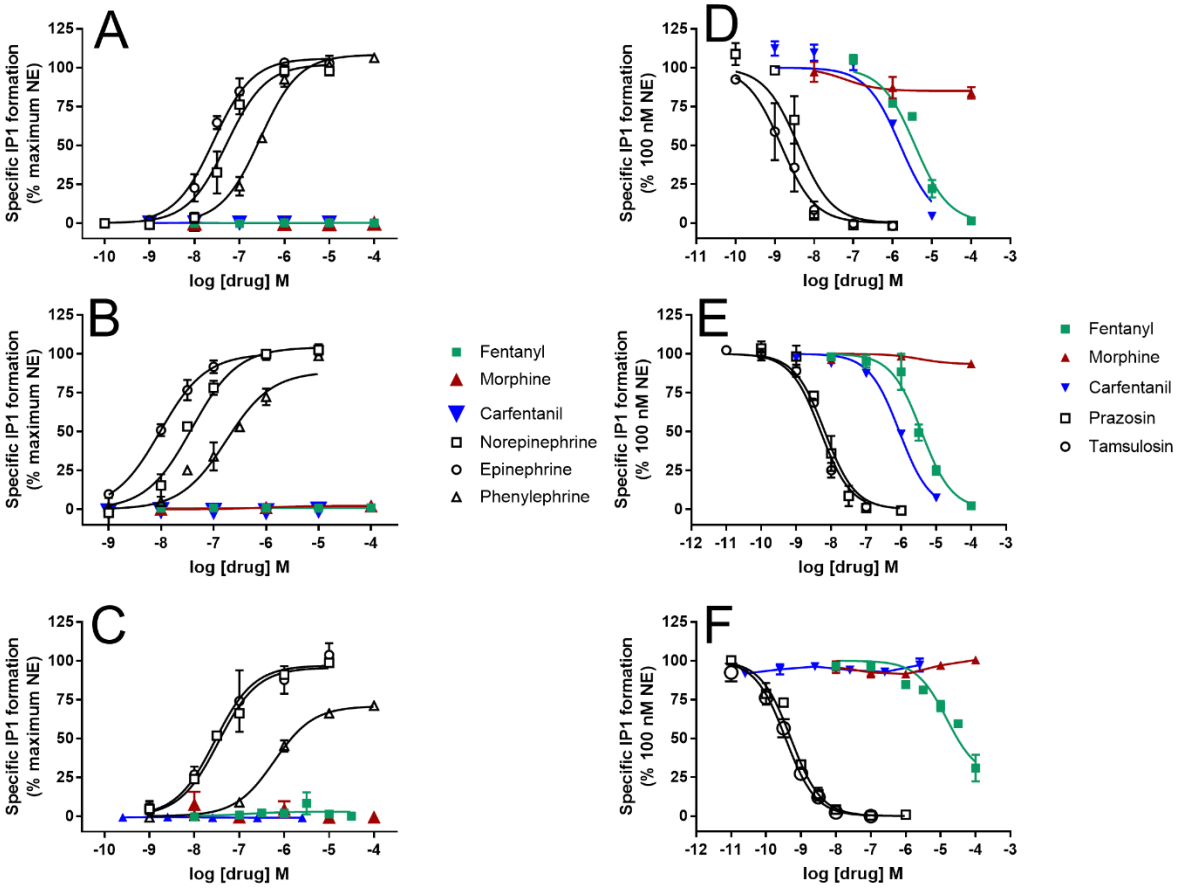

JPET Fast Forward. Published on June 8, 2020 as DOI: 10.1124/jpet.120.265561
This article has not been copyedited and formatted. The final version may differ from this version.

Figure 4

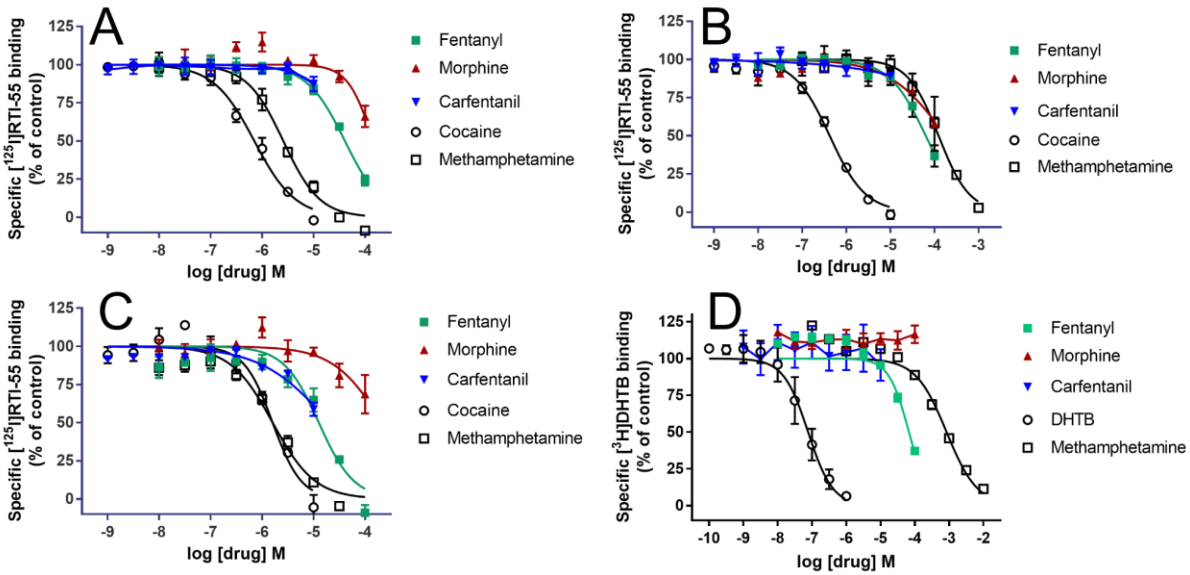

JPET Fast Forward. Published on June 8, 2020 as DOI: 10.1124/jpet.120.265561
This article has not been copyedited and formatted. The final version may differ from this version.

Figure 5

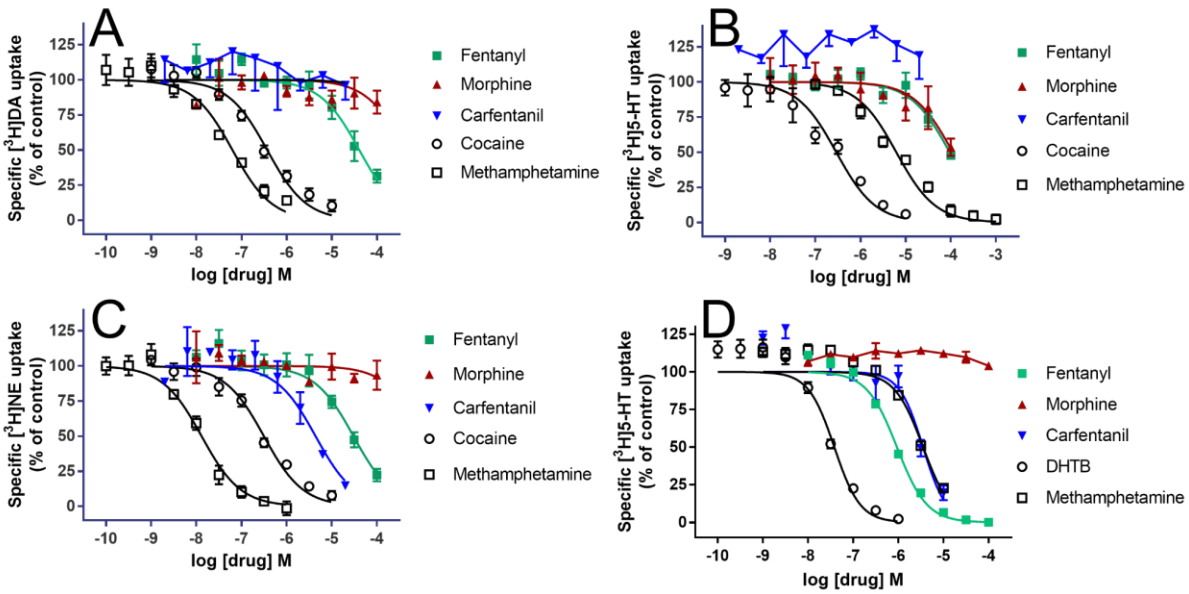

JPET Fast Forward. Published on June 8, 2020 as DOI: 10.1124/jpet.120.265561
This article has not been copyedited and formatted. The final version may differ from this version.

Figure 6.

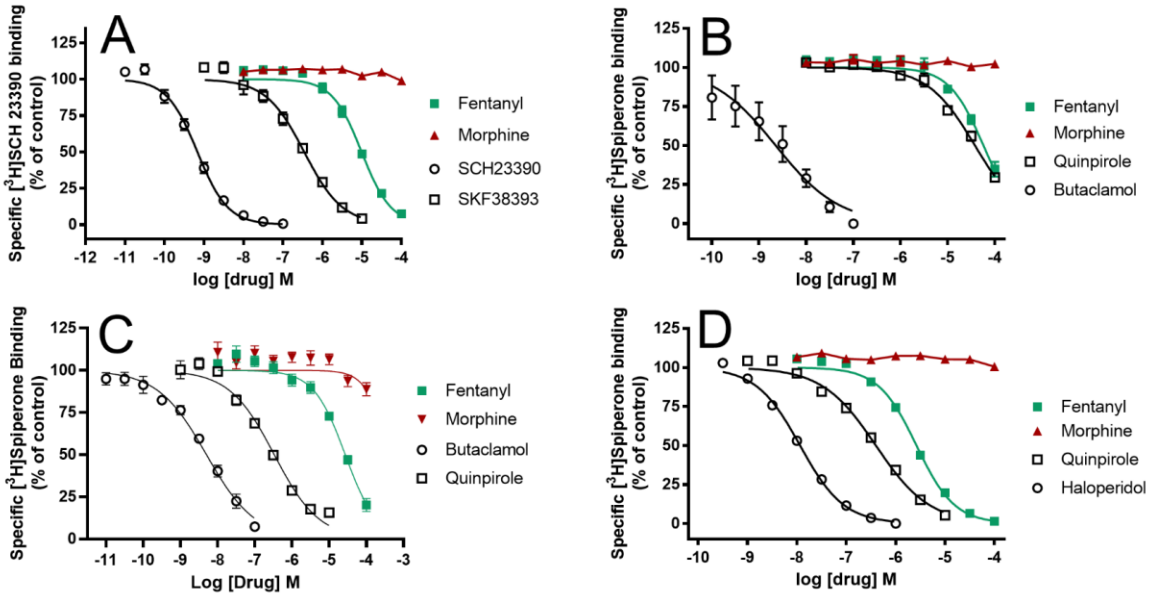

JPET Fast Forward. Published on June 8, 2020 as DOI: 10.1124/jpet.120.265561
This article has not been copyedited and formatted. The final version may differ from this version.

Figure 7

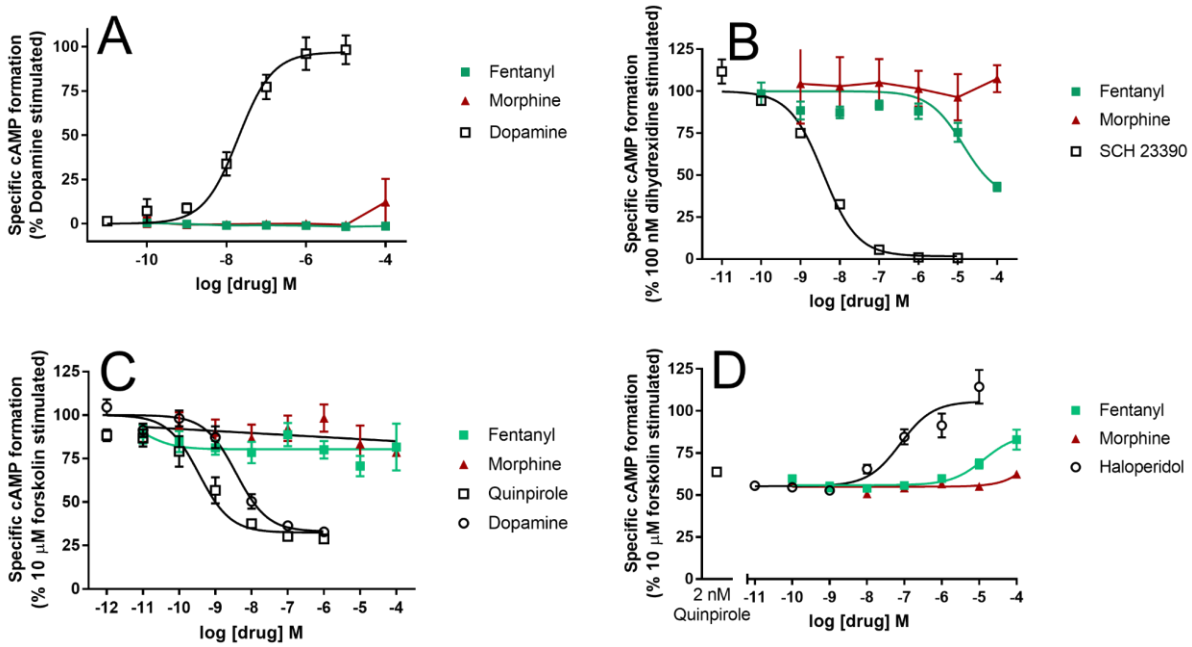

JPET Fast Forward. Published on June 8, 2020 as DOI: 10.1124/jpet.120.265561
This article has not been copyedited and formatted. The final version may differ from this version.

Figure 8

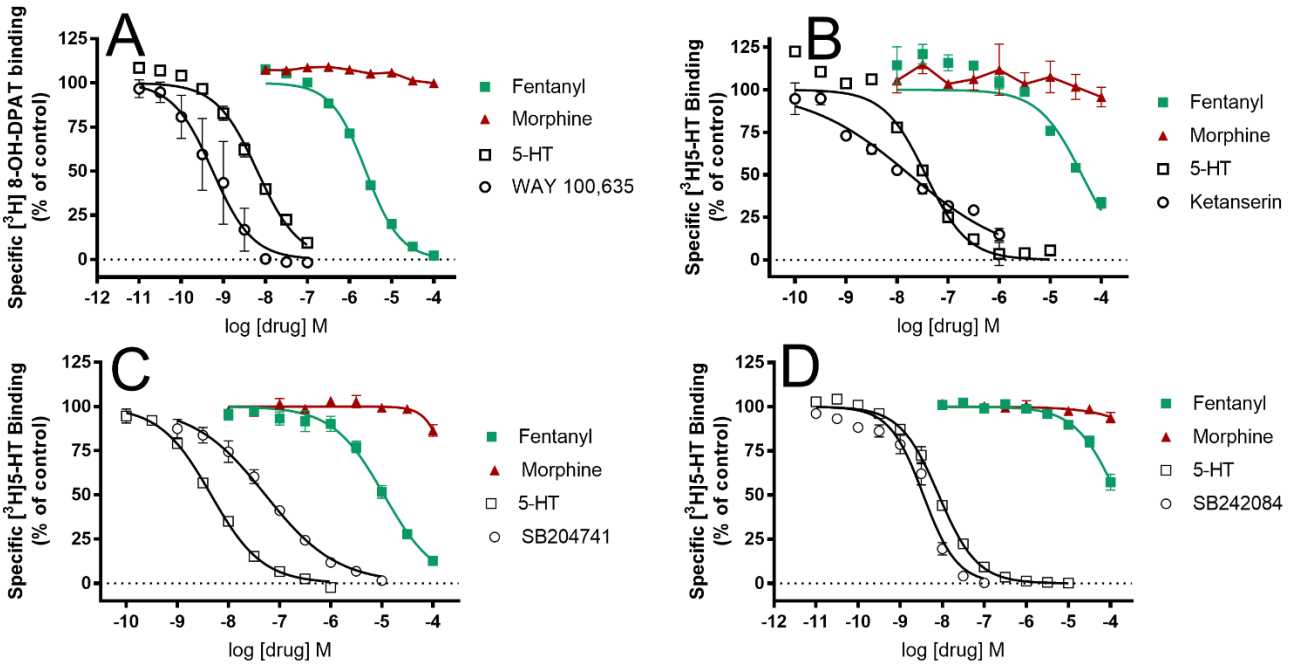

References

Aghajanian GK (1982) Central noradrenergic neurons: a locus for the functional interplay between alpha-2 adrenoceptors and opiate receptors. *J Clin Psychiatry* **43**:20-24.

Baumann MH, Kopajtic TA and Madras BK (2018) Pharmacological Research as a Key Component in Mitigating the Opioid Overdose Crisis. *Trends in pharmacological sciences* **39**:995-998.

Bennett JA, Abrams JT, Van Riper DF and Horrow JC (1997) Difficult or impossible ventilation after sufentanil-induced anesthesia is caused primarily by vocal cord closure. *Anesthesiology* **87**:1070-1074.

Bergstrom KA, Jolkkonen J, Kuikka JT, Akerman KK, Viinamaki H, Airaksinen O, Lansimies E and Tiihonen J (1998) Fentanyl decreases beta-CIT binding to the dopamine transporter. *Synapse (New York, NY)* **29**:413-415.

Bresink I, Danysz W, Parsons CG and Mutschler E (1995) Different binding affinities of NMDA receptor channel blockers in various brain regions--indication of NMDA receptor heterogeneity. *Neuropharmacology* **34**:533-540.

Burns G, DeRienz RT, Baker DD, Casavant M and Spiller HA (2016) Could chest wall rigidity be a factor in rapid death from illicit fentanyl abuse? *Clinical toxicology (Philadelphia, Pa)* **54**:420-423.

Cheng Y and Prusoff WH (1973) Relationship between the inhibition constant (K1) and the concentration of inhibitor which causes 50 per cent inhibition (I50) of an enzymatic reaction. *Biochem Pharmacol* **22**:3099-3108.

Chesser R, Pardi J, Concheiro M and Cooper G (2019) Distribution of synthetic opioids in postmortem blood, vitreous humor and brain. *Forensic Sci Int* **305**:109999.

Cozzi NV, Gopalakrishnan A, Anderson LL, Feih JT, Shulgin AT, Daley PF and Ruoho AE (2009) Dimethyltryptamine and other hallucinogenic tryptamines exhibit substrate behavior at the serotonin uptake transporter and the vesicle monoamine transporter. *J Neural Transm (Vienna)* **116**:1591-1599.

de Waal PW, Shi J, You E, Wang X, Melcher K, Jiang Y, Xu HE and Dickson BM (2020) Molecular mechanisms of fentanyl mediated β-arrestin biased signaling. *PLoS Comput Biol* **16**:e1007394.

Ebert B, Andersen S, Hjeds H and Dickenson AH (1998) Dextropropoxyphene acts as a noncompetitive N-methyl-D-aspartate antagonist. *Journal of pain and symptom management* **15**:269-274.

Erickson JD, Schafer MK, Bonner TI, Eiden LE and Weihe E (1996) Distinct pharmacological properties and distribution in neurons and endocrine cells of two isoforms of the human vesicular monoamine transporter. *Proc Natl Acad Sci U S A* **93**:5166-5171.

Eshleman AJ, Carmolli M, Cumbay M, Martens CR, Neve KA and Janowsky A (1999) Characteristics of drug interactions with recombinant biogenic amine transporters expressed in the same cell type. *J Pharmacol Exp Ther* **289**:877-885.

Eshleman AJ, Wolfrum KM, Hatfield MG, Johnson RA, Murphy KV and Janowsky A (2013) Substituted methcathinones differ in transporter and receptor interactions. *Biochem Pharmacol* **85**:1803-1815.

Eshleman AJ, Wolfrum KM, Reed JF, Kim SO, Johnson RA and Janowsky A (2018) Neurochemical pharmacology of psychoactive substituted N-benzylphenethylamines: High potency agonists at 5-HT2A receptors. *Biochem Pharmacol* **158**:27-34.

Farrens DL, Dunham TD, Fay JF, Dews IC, Caldwell J and Nauert B (2002) Design, expression, and characterization of a synthetic human cannabinoid receptor and cannabinoid receptor/ G-protein fusion protein. *The journal of peptide research : official journal of the American Peptide Society* **60**:336-347.

Fernandez-Fernandez C, Callado LF, Giron R, Sanchez E, Erdozain AM, Lopez-Moreno JA, Morales P, Rodriguez de Fonseca F, Fernandez-Ruiz J, Goya P, Meana JJ, Martin MI and Jagerovic N (2014) Combining rimonabant and fentanyl in a single entity: preparation and pharmacological results. *Drug design, development and therapy* **8**:263-277.

Fu MJ, Tsen LY, Lee TY, Lui PW and Chan SH (1997) Involvement of cerulospinal glutamatergic neurotransmission in fentanyl-induced muscular rigidity in the rat. *Anesthesiology* **87**:1450-1459.

Ge D, Yan X, Guo Y, Chen X, Guan R, Chen Y, Qiu D and Wang J (2015) Activation of alpha1-adrenoceptors facilitates excitatory inputs to medullary airway vagal preganglionic neurons. *J Appl Physiol (1985)* **119**:686-695.

Govoni S, Kumakura K, Spano PF, Tonon GC and Trabucchi M (1975) Interaction of narcotic analgesics with dopamine receptors in rat brain. *Pharmacological research communications* **07**:95-100.

Grant ER, Bacskai BJ, Pleasure DE, Pritchett DB, Gallagher MJ, Kendrick SJ, Kricka LJ and Lynch DR (1997) N-methyl-D-aspartate receptors expressed in a nonneuronal cell line mediate subunit-specific increases in free intracellular calcium. *The Journal of biological chemistry* **272**:647-656.

Grell FL, Koons RA and Denson JS (1970) Fentanyl in anesthesia: a report of 500 cases. *Anesthesia and analgesia* **49**:523-532.

Haxhiu MA, Kc P, Neziri B, Yamamoto BK, Ferguson DG and Massari VJ (2003) Catecholaminergic microcircuitry controlling the output of airway-related vagal preganglionic neurons. *J Appl Physiol (1985)* **94**:1999-2009.

Hedegaard HB, B. A.; Tinidad, J. P.; Spencer, M.; & Warner, M. (2018) Drugs Most Frequently Involved in Drug Overdose Deaths: United States, 2011-2016, in, National Center for Health Statistics, Hyattsville, MD.

Heiskanen T, Langel K, Gunnar T, Lillsunde P and Kalso EA (2015) Opioid Concentrations in Oral Fluid and Plasma in Cancer Patients With Pain. *Journal of pain and symptom management* **50**:524-532.

Hicks HC, Mowbray AG and Yhap EO (1981) Cardiovascular effects of and catecholamine responses to high dose fentanyl-O2 for induction of anesthesia in patients with ischemic coronary artery disease. *Anesthesia and analgesia* **60**:563-568.

Hustveit O (1994) Binding of fentanyl and pethidine to muscarinic receptors in rat brain. *Japanese journal of pharmacology* **64**:57-59.

Jannetto PJ, Helander A, Garg U, Janis GC, Goldberger B and Ketha H (2019) The Fentanyl Epidemic and Evolution of Fentanyl Analogs in the United States and the European Union. *Clinical chemistry* **65**:242-253.

Janowsky A, Eshleman AJ, Johnson RA, Wolfrum KM, Hinrichs DJ, Yang J, Zabriskie TM, Smilkstein MJ and Riscoe MK (2014) Mefloquine and psychotomimetics share neurotransmitter receptor and transporter interactions in vitro. *Psychopharmacology (Berl)* **231**:2771-2783.

Jensen BC, Swigart PM, Laden ME, DeMarco T, Hoopes C and Simpson PC (2009) The alpha-1D Is the predominant alpha-1-adrenergic receptor subtype in human epicardial coronary arteries. *Journal of the American College of Cardiology* **54**:1137-1145.

Jiwa N, Sheth H and Silverman R (2018) Naloxone-Induced Non-Cardiogenic Pulmonary Edema: A Case Report. *Drug safety - case reports* **5**:20.

Kalvass JC, Olson ER, Cassidy MP, Selley DE and Pollack GM (2007) Pharmacokinetics and pharmacodynamics of seven opioids in P-glycoprotein-competent mice: assessment of unbound

brain EC50,u and correlation of in vitro, preclinical, and clinical data. *J Pharmacol Exp Ther* **323**:346-355.

Katchman AN, McGroary KA, Kilborn MJ, Kornick CA, Manfredi PL, Woosley RL and Ebert SN (2002) Influence of opioid agonists on cardiac human ether-a-go-go-related gene K(+) currents. *J Pharmacol Exp Ther* **303**:688-694.

Lalley PM (2003a) μ-Opioid receptor agonist effects on medullary respiratory neurons in the cat: evidence for involvement in certain types of ventilatory disturbances. *American Journal of Physiology-Regulatory, Integrative and Comparative Physiology* **285(6)**:R1287-1304.

Lalley PM (2003b) Mu-opioid receptor agonist effects on medullary respiratory neurons in the cat: evidence for involvement in certain types of ventilatory disturbances. *American journal of physiology Regulatory, integrative and comparative physiology* **285**:R1287-1304.

Lalley PM (2005a) D1-dopamine receptor agonists prevent and reverse opiate depression of breathing but not antinociception in the cat. *American journal of physiology Regulatory, integrative and comparative physiology* **289**:R45-51.

Lalley PM (2005b) D1-dopamine receptor blockade slows respiratory rhythm and enhances opioid-mediated depression. *Respiratory physiology & neurobiology* **145**:13-22.

Lui PW, Chang GJ, Lee TY and Chan SH (1993) Antagonization of fentanyl-induced muscular rigidity by denervation of the coerulospinal noradrenergic pathway in the rat. *Neurosci Lett* **157**:145-148.

Lui PW, Lee TY and Chan SH (1989) Involvement of locus coeruleus and noradrenergic neurotransmission in fentanyl-induced muscular rigidity in the rat. *Neurosci Lett* **96**:114-119.

Lui PW, Lee TY and Chan SH (1990) Involvement of coerulospinal noradrenergic pathway in fentanyl-induced muscular rigidity in rats. *Neurosci Lett* **108**:183-188.

Lui PW, Tsen LY, Fu MJ, Yeh CP, Lee TY and Chan SH (1995) Inhibition by intrathecal prazosin but not yohimbine of fentanyl-induced muscular rigidity in the rat. *Neurosci Lett* **201**:167-170.

Martin DC, Introna RP and Aronstam RS (1991) Fentanyl and sufentanil inhibit agonist binding to 5-HT1A receptors in membranes from the rat brain. *Neuropharmacology* **30**:323-327.

McClain DA and Hug CC, Jr. (1980) Intravenous fentanyl kinetics. *Clinical pharmacology and therapeutics* **28**:106-114.

Peng PW and Sandler AN (1999) A review of the use of fentanyl analgesia in the management of acute pain in adults. *Anesthesiology* **90**:576-599.

Pertwee RG (2008a) The diverse CB1 and CB2 receptor pharmacology of three plant cannabinoids: delta9-tetrahydrocannabinol, cannabidiol and delta9-tetrahydrocannabivarin. *Br J Pharmacol* **153**:199-215.

Pertwee RG (2008b) Ligands that target cannabinoid receptors in the brain: from THC to anandamide and beyond. *Addiction biology* **13**:147-159.

Provencher BA, Eshleman AJ, Johnson RA, Shi X, Kryatova O, Nelson J, Tian J, Gonzalez M, Meltzer PC and Janowsky A (2018) Synthesis and Discovery of Arylpiperidinylquinazolines: New Inhibitors of the Vesicular Monoamine Transporter. *J Med Chem* **61**:9121-9131.

Ray WA, Chung CP, Murray KT, Hall K and Stein CM (2016) Prescription of Long-Acting Opioids and Mortality in Patients With Chronic Noncancer Pain. *Jama* **315**:2415-2423.

Rickli A, Liakoni E, Hoener MC and Liechti ME (2018) Opioid-induced inhibition of the human 5-HT and noradrenaline transporters in vitro: link to clinical reports of serotonin syndrome. *Br J Pharmacol* **175**:532-543.

Scamman FL (1983) Fentanyl-O2-N2O rigidity and pulmonary compliance. *Anesthesia and analgesia* **62**:332-334.

Shi X, Walter NA, Harkness JH, Neve KA, Williams RW, Lu L, Belknap JK, Eshleman AJ, Phillips TJ and Janowsky A (2016) Genetic Polymorphisms Affect Mouse and Human Trace Amine-Associated Receptor 1 Function. *PLoS One* **11**:e0152581.

Slavova S, Costich JF, Bunn TL, Luu H, Singleton M, Hargrove SL, Triplett JS, Quesinberry D, Ralston W and Ingram V (2017) Heroin and fentanyl overdoses in Kentucky: Epidemiology and surveillance. *The International journal on drug policy* **46**:120-129.

Sohn JT, Ding X, McCune DF, Perez DM and Murray PA (2005) Fentanyl attenuates alpha1B-adrenoceptor-mediated pulmonary artery contraction. *Anesthesiology* **103**:327-334.

Sokoll MD, Hoyt JL and Gergis SD (1972) Studies in muscle rigidity, nitrous oxide, and narcotic analgesic agents. *Anesthesia and analgesia* **51**:16-20.

Somerville NJ, O'Donnell J, Gladden RM, Zibbell JE, Green TC, Younkin M, Ruiz S, Babakhanlou-Chase H, Chan M, Callis BP, Kuramoto-Crawford J, Nields HM and Walley AY (2017) Characteristics of Fentanyl Overdose - Massachusetts, 2014-2016. *MMWR Morbidity and mortality weekly report* **66**:382-386.

Stanley TH (2014) The fentanyl story. *The journal of pain : official journal of the American Pain Society* **15**:1215-1226.

Stone DJ and DiFazio CA (1988) Anesthetic action of opiates: correlations of lipid solubility and spectral edge. *Anesthesia and analgesia* **67**:663-666.

Streisand JB, Bailey PL, LeMaire L, Ashburn MA, Tarver SD, Varvel J and Stanley TH (1993) Fentanyl-induced rigidity and unconsciousness in human volunteers. Incidence, duration, and plasma concentrations. *Anesthesiology* **78**:629-634.

Thomson IR, Hudson RJ, Rosenbloom M and Torchia MG (1988) Catecholamine responses to anesthetic induction with fentanyl and sufentanil. *J Cardiothorac Anesth* **2**:18-22.

Torralva R and Janowsky A (2019) Noradrenergic Mechanisms in Fentanyl-Mediated Rapid Death Explain Failure of Naloxone in the Opioid Crisis. *J Pharmacol Exp Ther* **371**:453-475.

Traynor JR and Nahorski SR (1995) Modulation by mu-opioid agonists of guanosine-5'-O-(3-[35S]thio)triphosphate binding to membranes from human neuroblastoma SH-SY5Y cells. *Mol Pharmacol* **47**:848-854.

Tschirhart JN, Li W, Guo J and Zhang S (2019) Blockade of the Human Ether A-Go-Go-Related Gene (hERG) Potassium Channel by Fentanyl. *Mol Pharmacol* **95**:386-397.

Tsou MY, Lui PW, Lee TY, Pan JT and Chan SH (1989) Differential effects of prazosin and yohimbine on fentanyl-induced muscular rigidity in rats. *Neuropharmacology* **28**:1163-1168.

Upton RN (1996) A model of the first pass passage of drugs from i.v. injection site to the heart--parameter estimates for lignocaine in the sheep. *Br J Anaesth* **77**:764-772.

Vasudevan L, Vandeputte M, Deventer M, Wouters E, Cannaert A and Stove CP (2020) Assessment of structure-activity relationships and biased agonism at the Mu opioid receptor of novel synthetic opioids using a novel, stable bio-assay platform. *Biochem Pharmacol* **177**:113910.

Willette RN and Sapru HN (1982) Pulmonary opiate receptor activation evokes a cardiorespiratory reflex. *European journal of pharmacology* **78**:61-70.

Yamakura T, Sakimura K and Shimoji K (1999) Direct inhibition of the N-methyl-D-aspartate receptor channel by high concentrations of opioids. *Anesthesiology* **91**:1053-1063.

Yamanoue T, Brum JM, Estafanous FG, Khairallah PA and Ferrario CM (1993) Fentanyl attenuates porcine coronary arterial contraction through M3-muscarinic antagonism. *Anesthesia and analgesia* **76**:382-390.

Yang M, Reese J, Cotecchia S and Michel MC (1998) Murine alpha1-adrenoceptor subtypes. I. Radioligand binding studies. *J Pharmacol Exp Ther* **286**:841-847.

Yasuda I, Hirano T, Yusa T and Satoh M (1978) Tracheal constriction by morphine and by fentanyl in man. *Anesthesiology* **49**:117-119.